TABLE OF CONTENTS

Topics **Page**

1.0. INTRODUCTION

1.1. Dengue virus

Dengue is a vector-borne disease which is transmitted by mosquitos. The Dengue virus belongs to the family *Flaviviridae* with the genus *Flavivirus*. The vectors that are mainly responsible in transmitting Dengue to humans is mainly *Aedes aegypti* and *Aedes albopictus*. To date the strategy of Dengue control focuses on vector control and real-time monitoring. Dengue virus infection carries a complex system of the antibody-dependent enhancement and original antigen sin as reported by McMichael (1998) that makes development of a vaccine very challenging. Prior exposure to one of the four serotypes can increase the probability of a persons' immune system boosts the viral infection. In addition, it is possible to develop into potentially lethal Dengue Haemorrhaging Fever (DHF) or Dengue Shock Syndrome (DSS) who have already recovered from the infection of another serotype. Thus, there is a need to design and develop broad range anti-viral drug that is able to inhibit the replication of Dengue viruses.

The Dengue virus serine protease is largely involved in the viral replication process and it is a promising target for drug development. There are four serotypes of Dengue virus, namely DEN1, DEN2, DEN3 and DEN4. However, currently only DEN3 protease crystal structure with bound inhibitor (aprotinin) has been elucidated (Noble, et. al, 2012). On-going work in our research lab has been dealing with DEN2 serine protease. Hence, this project aims in performing structural comparison between the homology model of DEN2 and the crystal structure of DEN3 NS2B-NS3 serine proteases.

1.2. Viral polyprotein

The viral genetic makeup is a single-stranded positive-sense RNA which encodes for a single polyprotein. As described by Wang, Q.-Y. et. al, (2009), the Flavivirus are enveloped viruses having two outer membrane proteins, the envelope (E) and the membrane (M) processed from the precursor prM. The single polyprotein is thought to be consisting of three structural proteins which are C, prM and E and seven Non-structural proteins.

Figure 1. The DENV (+) RNA genome and the co-linear polyprotein.

The seven Non-structural proteins are NS1, NS2A, NS2B, NS3, NS4A, NS4B and NS5. Non-structural protein NS2B-NS3 serine protease is one of the drug targets because it is essential for the viral growth and also exhibits enzymatic activity. The single polyprotein that is translated from its genome is subjected to cleaving mechanisms of the host cellular proteases and a viral serine protease made of NS2B and NS3 (protease N-terminus domain). The enzymatic properties of the serine protease enable it to be targeted in drug screening within the drug discovery pipeline. NS3 protein carries two functional domains, an N-terminal serine protease which is around 170 amino acids long and a C-terminus helicase or a RNA triphosphatase which is about 440 amino acid in length (Lee et. al, 2007; Othman et al., 2008). The protease domain is inactive and requires a 40 amino acid chain of NS2B cofactor to be bound to form a protease active site. The NS2B-NS3 protease has been the first dengue protein target actively used in drug discovery and developments (Falgout et. al, 1991).

2.0. LITERATURE REVIEW

Computational tools could be used to help design and study the binding interactions in order to carefully select the hits with the highest potency. These tools are mainly used in high throughput screening (HTS) method in early drug discovery programs to evaluate and select highly specific small peptides or ligands against a particular target of interest. There are many docking software available, one of the popular docking tool is Autodock provided by The Scripps Research Institute. It is developed to predict the binding interaction of small peptides (ligands) onto the 3-dimensional (3D) macromolecule structure (Huey et al, 2009). Molecular docking tools such as Autodock tools has been reported to use the energy of binding to correctly select the protein-ligand complexes without prior knowledge of the binding pockets. It is also proven to be efficient and robust in automating the search of the binding sites and ligand orientations (Hetenyi et al., 2002). Molecular docking was used for drug designing about 26 years ago, combining the computational methods which employs a search algorithm to generate the binding mode prediction of a ligand onto its specific receptor target. This binding modes coupled with its scoring function enables the ranking and selection of the most probable ligand binding interactions (Barril, et al, 2005).

3-dimensional (3D) structures of the proteins have been able to assist the computer aided drug design. Elucidated protein structures can be obtained from the Protein Data Bank and used for comparative structural analysis and structure activity relationship predictions. The structure of interest in this study is the Dengue virus NS2B-NS3 serine protease complex. The dengue virus NS2B-NS3 plays an important role in proteolytic processing of the viral polyprotein. The NS3 protease was reported to be having a trypsin-like serine protease domain with histidine, aspartic acid and serine residues at its

active site (Bazan et al, 1989; Lee et. al., 2007; Othman et. al., 2008; Tomlinson et. al, 2011).

The structure activity relationship study on the dengue virus serine protease with the inhibitors could provide useful information in designing an inhibitor which has the potency to develop into an anti-dengue drug (Othman et. al., 2008). Several identified natural compounds have shown to have inhibitory activity on the dengue virus NS2B-NS3 protease. 4-hydroxypanduratin A is a competitive inhibitor which binds to the active site of the serine protease. The hydrophobic pockets which are formed by Val52, Leu128, Pro132 anad Val155 allows docking of the competitive inhibitor. This competitive inhibitor is also reported to form hydrogen bonds with Ser135 and Gly151 (Lee et. al., 2007).

For the non-competitive inhibitors (alpinetin, pinocembrin, pinostrobin and cardamonin), their binding site is expected not to be at the active site. They bind to a similar allosteric site on the dengue virus type 2 (Othman et. al., 2008). These findings could be compared with the recently published DEN3 NS2B-NS3 crystal structure and analyse the interaction involved between them. Hence, the ligands used in this study involve competitive and non-competitive inhibitors (ligands). Molecular docking of DEN2 homology model and DEN3 NS2B-NS3 serine proteases were docked with competitive (4-hydroxypanduratin A) and non-competitive inhibitors (alpinetin, pinocembrin, pinostrobin and cardamonin).

3.0. OBJECTIVES AND AIMS

3.1. Objectives

The objectives of the project are,

(i) to align and compare the structures of DEN2 (homology model) and DEN3 (crystal) NS2B-NS3 serine proteases,

(ii) to dock (computational) competitive and non-competitive inhibitors into the DEN2 and DEN3 serine proteases, and

(iii) to analyse and compare the binding interactions between the inhibitors and the respective serine proteases.

3.2. Aims

Aim of the research project is to investigate the binding interactions involved between the competitive inhibitor (4-hydroxypanduratin A) and non-competitive inhibitors (alpinetin, pinocembrin, pinostrobin and cardamonin) with DEN2 NS2B-NS3 2FOMP7 homology model and DEN3 NS2B-NS3 proteases crystal structures.

4.0. METHODOLOGY

4.1. Preparation of protein and ligand structures input files

The methods involved in this study include: building the input files, docking of ligands to proteins using Autodock v.4.2 and analysing the binding interactions using softwares such as the Discovery Studio Visualiser v.3.1 and the Ligplot program. Binding interactions of the competitive and non-competitive inhibitors highlighted in this study can help to determine whether these compounds, besides DEN2 NS2B-NS3 serine proteases, can also able to inhibit other Dengue virus serotypes such as DEN3. Hence, information obtained from this study can aid towards designing optimized inhibitors for the different serotypes of Dengue virus serine proteases.

The DEN2 NS2B-NS3 homology model, 2FOMP7 (provided by Choon Han) and the DEN3 NS2B-NS3 serine proteases input files was prepared and saved in PDBQT format for use with Autodock. The published three-dimensional (3D) structures of DEN3 NS2B-NS3 serine protease was obtained from Protein Data Bank (http://www.rcsb.org/pdb/home; accession code: 3U1I and 3U1J). 3U1I structure is bound to peptide inhibitor (two cascade structures separated into 3U1I_1 and 3U1I_2) and 3U1J is aprotinin bound (Resolution[Å]: 1.80). Sulphate ions and water were removed and saved as PDB file. The inhibitors (competitive inhibitor: hydroxypanduratin A, and non-competitive inhibitors: alpinetin, pinocembrin, pinostrobin and cardamonin) structures were obtained from PubChem (http://pubchem.ncbi.nlm.nih.gov/).

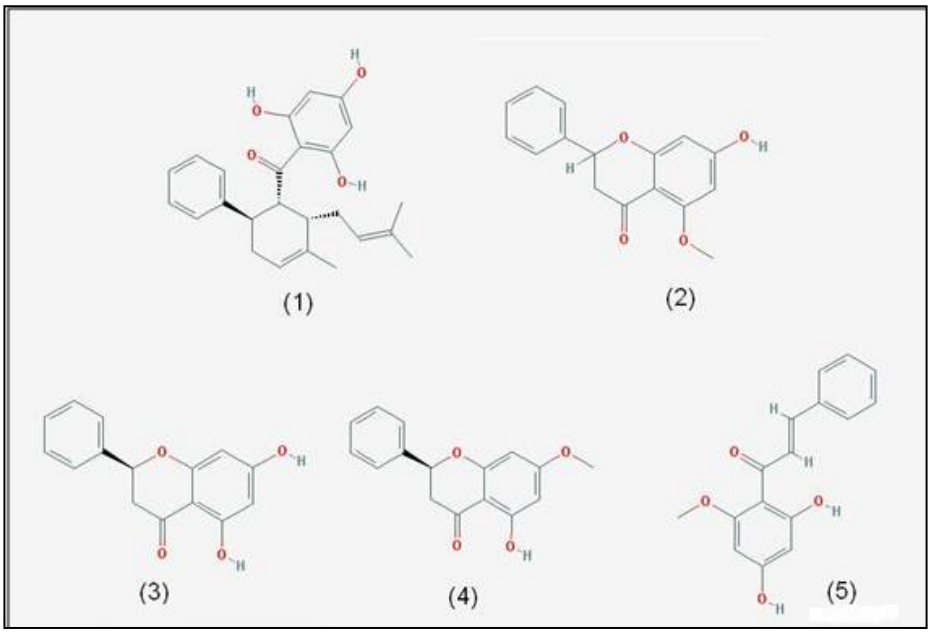

Figure 2: 2D structures of inhibitors; Key: 1 – 4-hydoxypanduratin A*, 2 – alpinetin, 3 – pinocembrin, 4 – pinostrobin, 5 –cardamonin. *competitive inhibitor

These inhibitors (ligands) used in this study are found to be isolated from *Boesenbergia rotunda L.* and have shown inhibitory activity towards the Dengue virus type 2 protease and other *Flaviruses* (Lee, 2007; Othman, 2008). Competitive inhibitor is 4-hydroxypanduratin A and the non-competitive inhibitors are alpinetin, pinocembrin, pinostrobin and cardamonin.

4.2. Alignment and comparison of protein structures

Structural alignment was performed to compare the protein structures (2FOMP7, 3U1I_1, 3U1I_2 and 3UIJ) using Discovery Studio 3.0 Visualiser (Accelrys Software Inc.). These protein structures were aligned using custom tethering on the reported catalytic triad (HIS51, ASP75 and SER135) of the dengue virus serine protease (Othman et al, 2008).

4.3. Molecular docking of competitive and non-competitive inhibitors

The molecular docking of protein macromolecules and ligands (competitive and non-competitive inhibitors) were performed using Autodock v.4.5. Docking files were prepared using the aforementioned Autodock software. Protein molecules were prepared by adding polar hydrogens and the non-polar hydrogens are merged. Kollman charges were added to the protein molecule and Gasteiger charges assigned. The solvation parameters were assigned by default. For the ligands, hydrogen atoms were added. All rotatable bonds of ligands were set to be rotatable by default. Both the macromolecule (protein) and ligand files are saved in PDBQT format.

Docking was performed using genetic algorithm (GA) and local search methods. A population size of 150 and 250,000 energy evaluations were used for 100 times searches, with a 70 x 70 x 70 dimension of grid box size (competitive inhibitors), 126 x 100 x 116 dimension of grid box size (non-competitive inhibitors) and 0.375 Å grid spacing around the catalytic triad for the competitive inhibitors (His51, Asp75 and Ser135). The grid box was centered to the macromolecule. Clustering histogram analyses were done to choose the best conformer model. The best conformations were chosen from the lowest docked energy which populate the highest number of molecules in a particular cluster. The Hydrogen bond, van der Waals and hydrophobic interactions were analysed using Ligplot and Discovery Studio 3.0 Visualiser (Accelrys Software Inc.). Autodock required the Docking Parameter File (*.dpf) to be prepared with the parameters mention earlier to perform the docking process (Appendix 1).

Interactions between enzyme and ligands were calculated by using docked energies. The energies obtained from the docking calculations include intermolecular and intramolecular interaction energies. Autodock provides a report of the final docked

energies for each run according to its energy function for the docked structures. Prior to setting up the Autodock, the Grid Parameter File (*.gpf) (Appendix 3) was required as Autogrid calculates the non-covalent energy of interaction between the receptor and the probe atom that is located in the different grid points. Autogrid builds the files required as many as the number of probe atoms used. The probes are usually the atoms present in the ligands that will be docked onto the receptor to generate the affinity grid maps of the given receptor molecule.

Docking process was performed using the generated grid maps in Autodock software package. The cluster histogram was analysed using the generated Docking Log file (*.dlg). Conformation with the lowest docked energy was chosen from the most populated cluster (Appendix 3).

5.0. RESULTS

5.1. Structural alignment

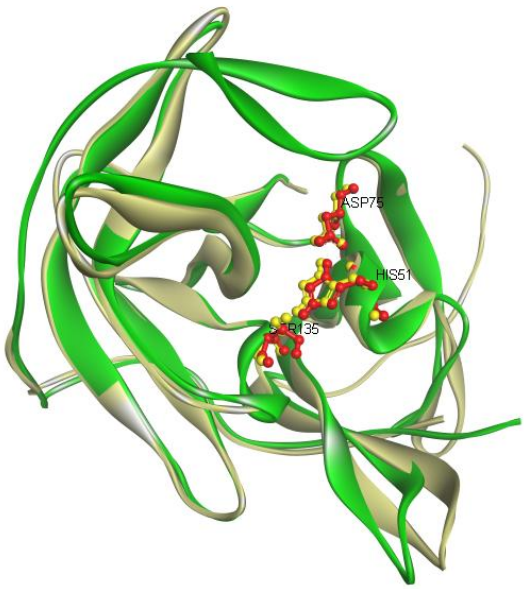

Figure 3: (a) Structural alignment between 2FOMP7 (green) and 3U1J (light yellow). Catalytic triad coloured in red for 2FOMP7 and 3U1J is yellow, shown as ball and stick.

Structural alignment by protein tethering superimpose was performed at the HIS51, ASP75 and SER135 on the NS3 chain residues using Discovery Studio 3.1 Visualiser (Figure 3.1.). The superimposition was performed on the DEN2 NS2B-NS3 2FOMP7 homology model and the DEN3 crystal structures. The distance of the catalytic triad between 2FOMP7 and 3U1J NS2B-NS3 serine protease is 1.16 Å. The similarities between the structures compared in this study were between 0.5 to 1.16 Å as shown in Table 3.1.

The superimposition shows the structures of the NS2B-NS3 protease are identical. Multiple alignment of the structure sequences using the PDBe Fold v.2.51 (EBI) further shows that the structures are identical with an overall RMSD 0.7573 (Table 3.2). Table 3.2 shows the RMSD, Q-score and sequence identiy of the protease structures.

However, structural superimposition between 2FOMP7 and 3U1J showed some residue differences at the loop regions away from the active site. As reported by Chandramouli et al. (2010) the Dengue protease has highly conserved regions around the catalytic triad across the serotypes, similarities are reported to be more than 63%. These conserved regions are highly conserved across the *Flavivirus* and it gives the scope of flexibility for the development of a broad spectrum drugs.

Protein	2FOMP7	3U1J	3U1I_1	3U1I_2
2FOMP7	-	1.1616	1.1535	1.0130
3U1J	1.1616	-	0.8754	0.6077
3U1I_1	1.1535	0.8754	-	0.5131
3U1I_2	1.0130	0.6077	0.5131	-

Table 3.1.: Comparison of RMSD values of superimpose by tethering catalytic triad of NS2B-NS3 serine proteases structures.

##	Structure	N_{res}	N_{SSE}	Consensus scores	
				RMSD	Q-score
1	2FOMP7.pdbqt:B	152	14	0.5270	0.9509
2	3U1I_1.pdbqt:D	165	16	0.3940	0.8877
3	3U1I_2.pdbqt:B	168	16	0.3882	0.8723
4	3U1J.pdbqt:B	166	15	0.5258	0.8708

Number of aligned residues	149	Overall RMSD	0.7573
Number of aligned SSEs	12	Overall Q-score	0.8173

Cross-structure statistics

RMSD

	structure:	1	2	3	4
1	2FOMP7.pdbqt:B	-	0.758	0.808	0.862
2	3U1I_1.pdbqt:D	0.758	-	0.497	0.812
3	3U1I_2.pdbqt:B	0.808	0.497	-	0.751
4	3U1J.pdbqt:B	0.862	0.812	0.751	-

Q-score

	structure:	1	2	3	4
1	2FOMP7.pdbqt:B	-	0.832	0.811	0.813
2	3U1I_1.pdbqt:D	0.832	-	0.780	0.755
3	3U1I_2.pdbqt:B	0.811	0.780	-	0.749
4	3U1J.pdbqt:B	0.813	0.755	0.749	-

Sequence Identity

	structure:	1	2	3	4
1	2FOMP7.pdbqt:B	-	0.698	0.698	0.698
2	3U1I_1.pdbqt:D	0.698	-	1.000	1.000
3	3U1I_2.pdbqt:B	0.698	1.000	-	1.000
4	3U1J.pdbqt:B	0.698	1.000	1.000	-

Table 3.2.: Multiple alignment results using PDBe Fold v2.51, EBI.

5.2. Molecular Docking

Molecular docking process was initiated with a flexible ligand to obtain the best possible docked conformation on the macromolecule. The best conformer docked model of the ligand onto the DEN 2FOMP7 homology model, 3U1J, 3U1I_1 and 3U1I_2 was chosen based on the highest cluster number with the lowest binding energy. Higher cluster number was chosen as the main selection criteria as it gives higher possibility of the binding mode being most likely to be docked onto the protease. These clustering of the ligand docking are selected based on the default root mean square tolerance (rmstol) of 2.0 Å. The Autodock 4.2 clustering histogram output however ranks the ligand docking results based on the lowest binding energy. Figure 4 shows an example of the clustering histogram output from Autodock 4.2 upon completion of the docking process. The conformer docked complex was chosen for each ligand with the corresponding protease and analysed for the binding interaction using Accerlys Discovery 3.1 Visualiser and Ligplot software.

```
Outputting structurally similar clusters, ranked in order of increasing energy.


_____________________________________________________________________

Number of distinct conformational clusters found = 11,  out of 100 runs,
Using an rmsd-tolerance of 2.0 A


      CLUSTERING HISTOGRAM
      ____________________

_____________________________________________________________________
     |           |     |           |     |
Clus | Lowest    | Run | Mean      | Num | Histogram
-ter | Binding   |     | Binding   | in  |
Rank | Energy    |     | Energy    | Clus|    5    10   15   20   25   30   35
_____|___________|_____|___________|_____|____:____|____:____|____:____|____:___
   1 |     -7.52 |  96 |     -6.97 |  64 |#################################################################
   2 |     -7.31 |  87 |     -6.54 |   5 |#####
   3 |     -6.92 |  85 |     -6.66 |  14 |##############
   4 |     -6.85 |  99 |     -6.49 |   5 |#####
   5 |     -6.56 |   9 |     -6.56 |   1 |#
   6 |     -6.52 |  30 |     -6.46 |   3 |###
   7 |     -6.39 |  68 |     -6.39 |   1 |#
   8 |     -6.25 |   2 |     -6.19 |   2 |##
   9 |     -6.16 |  16 |     -6.01 |   2 |##
  10 |     -5.69 |  71 |     -5.69 |   1 |#
  11 |     -5.58 |  29 |     -5.56 |   2 |##
_____|___________|_____|___________|_____|_____________________________________
```

Figure 4: Example of the Autodock 4.2 clustering histogram output

5.2.1. Automated docking of competitive and non-competitive inhibitors

Tabulated molecular docking data show the comparison of the calculated free energy of binding, and K_i values. It is observed that the estimated free energy of binding for the DEN2 2FOMP7 homology model is higher compared to the other DEN3 serine proteases structure for the ligands used in this study (Table 3.3 and Table 3.4). The estimated inhibition constant, Ki (µM) is also noted to be higher for the DEN2 NS2B-NS3 2FOMP7 compared to the DEN3 NS2B-NS3 3UJ, 3U1_I and 3U1I_2 structures for all the ligands used in this study.

Table 3.3.: Comparison of free energy of binding values (kcal/mol) of docked conformer of the ligands to DEN2 homology model, DEN3 NS2B-NS3 proteases complex calculated using Autodock 4.2.

	Estimated free energy of binding (kcal/mol)			
Ligands	2FOMP7	3U1J	3U1I_1	3U1I_2
4-hydroxypanduratin A*	-3.72	-7.44	-7.56	-6.81
Alpinetin	-5.14	-6.52	-6.64	-7.11
Pinocembrin	-4.48	-7.94	-6.24	-5.94
Pinostrobin	-3.60	-6.83	-6.34	-6.35
Cardamonin	-4.7	-6.94	-6.2	-7.31

*competitive inhibitor

Table 3.4.: Comparison of Estimated inhibition constant, Ki (µM) of docked conformer of the ligands to DEN2 homology model, DEN3 NS2B-NS3 proteases complex calculated using Autodock 4.2.

	Estimated inhibition constant, Ki (µM)			
Ligands	2FOMP7	3U1J	3U1I_1	3U1I_2
4-hydroxypanduratin A*	1870	3.5	2.86	10.19
Alpinetin	170.17	16.7	13.55	6.15
Pinocembrin	516.09	1.51	26.76	44.43
Pinostrobin	2280	9.8	22.64	21.99
Cardamonin	356.63	8.16	28.54	4.37

*competitive inhibitor

Previously, reported value of binding energy for the 4-hydroxypanduratin A was -7.4 kcal/mol predicted using the same ligand on the catalytic triad of DEN2 NS2B-NS3 protease (Lee at al., 2007). Here in this study, DEN2 2FOMP7 homology model showed higher binding energy with the 4-hydroxypanduratin A (-3.72 kcal/mol). In addition, the other DEN3 crystal structures, 3U1J, 3U1I_1 and 3U1I_2 showed similar binding energy of -7.44, -7.5, -6.81 kcal/mol respectively and corresponding estimated inhibition value, Ki (µM) is also lower for the 4-hydroxypanduratin A. DEN3 NS2B-NS3 crystal structures showed comparatively lower estimated binding energy compared to DEN2 2FOMP7 homology model.

5.3. Binding interactions

There are several types of binding interactions and factors involved in a ligand-receptor binding. Alberty (2003) discussed that $\Delta G_{binding}$ equation is usually used to discuss the ligand-receptor binding. This equation encompasses desolvation of both ligand and receptor complex formation and direct contact interaction of free energy of the ligand on its receptor. The direct contact interactions involve van der Waals interactions, electrostatic interactions, and hydrogen bonds. Other factors to include are the conformational change and entropy loss upon formation of the complex. Hydrogen bonding (H-bond), van der Waals interactions and hydrophobic interactions are analysed for the docked conformer molecules in this study to further illustrate the important residues that governs the catalytic triad activity of the protease. Summary of the amino acid residues and their binding properties are summarised in Table 3.5. The hydrogen bonds and van der Waals interactions were determined using Accerlys Discovery Studio Visualiser. Figure 75– 9 shows the hydrogen bonding interactions for the respective ligands.

Table 3.5.: Summary of residues of DENV protease involved in hydrogen bonding, hydrophobic interactions and van der Waals interactions with the ligands

Ligand		Binding residues		
		H-bond	Hydrophobic interaction	van der Waals
4-HPA	2FOMP7	Ser131, Asp129	Pro132, Tyr150, Gly151, Tyr161	Ser135, Thr134, Tyr150, Gly151, Tyr161
	3U1J	His51, Ser135, Gly133, Thr134, Tyr150, Gly151	Val36, Pro132	Val36, Pro132
	3U1I_1	Gly133, Thr134, Ser135	Pro132, Gly133, Tyr150, Gly151, Tyr161	Asp129, Phe130, Tyr150, Gly151, Gly153, Tyr161
	3U1I_2	His51, Ser135, Gly151	Phe130, Lys131, Pro132, Gly133, Thr134, Tyr150, Tyr161	Val36, Asp129, Phe130, Lys131, Pro132, Gly133, Thr134, Tyr150

Alpinetin	2FOMP7	Asn152, Asn167	Lys73, Lys74, Ile78, Met84, Ala164, Ala166	Ile78, Met84, Ala164, Ala166
	3U1J	Gln35, Gly133	Val36, His51, Pro132, Ser135, Tyr150, Gly151	Val52, Lys131, Pro132, Thr134, Tyr150, Gly151, Tyr161
	3U1I_1	Gly133, Tyr150	Val36, His51, Pro132, Thr134, Tyr150, Tyr161	Val36, Pro132
	3U1I_2	Gly133, Thr134	Val36, His51, Val52, Phe130, Lys131, Pro132, Thr134, Ser135, Tyr150, Tyr161	Val36, Val52, Asp129, Pro132, Tyr161
Pinocembrin	2FOMP7	His51, Phe130, Ser131, Ser135, Thr134	Ile36, Ser131, Pro132, Tyr150, Tyr161	Ile36
	3U1J	Trp89, Gly124, Ile165, Gly167	Lys91, Thr115, Glu122, Ile123, Gln167	Lys91, Thr115, Glu122, Ile123,
	3U1I_1	Met84, Asn152, Gly153	Trp50, Asp75, Gly82, Thr83, Asn152, Tyr161	His51, Arg54, Asp75, Asp81, Thr83, Val155
	3U1I_2	Gly133, Thr134, Ser135,	Asp129,Phe130, Lys131,Pro132	Pro132
Pinostrobin	2FOMP7	Gly153	Pro132, Ser135, Tyr150, Gly151, Val155, Tyr161	His51, Phe130, Pro132, Ser131, Thr134, Ser135, Tyr150, Val155
	3U1J	Gln88, Gly124, Ile165	Trp89, Lys91, Glu122, Ile123, Gln167, Thr168	Trp89, Lys91, Ile123, Asn169, Thr168
	3U1I_1	Gly133, Thr134, Ser135, Tyr150	Tyr150, Val155, Tyr161	Val36, Pro132, Val155, Tyr161
	3U1I_2	Gly133, Gly151	Val36, His51, Phe130, Lys131, Pro132, Thr134, Ser135, Tyr150	Val36, Pro132
Cardamonin	2FOMP7	His51, Phe130, Ser131, Thr134, Gly151,	Ser131, Pro132, Ser135, Gly151, Tyr161	-
	3U1J	Asp129, Phe130, Gly133, Ser135,	His51, Pro132, Tyr150, Tyr161	Tyr161
	3U1I_1	Met84, Asn152, Gly151, Tyr161	Thr83, Arg85, Ile86, Asn152, Val154, Val155	Arg85, Thr83, Ile86, Val154, Val155
	3U1I_2	Gln88, Trp89, Gly124, Ile165,	Lys91, Glu122, Ile123, Ile165	Lys91, Glu122, Ile123

5.3.1. Hydrogen bonding

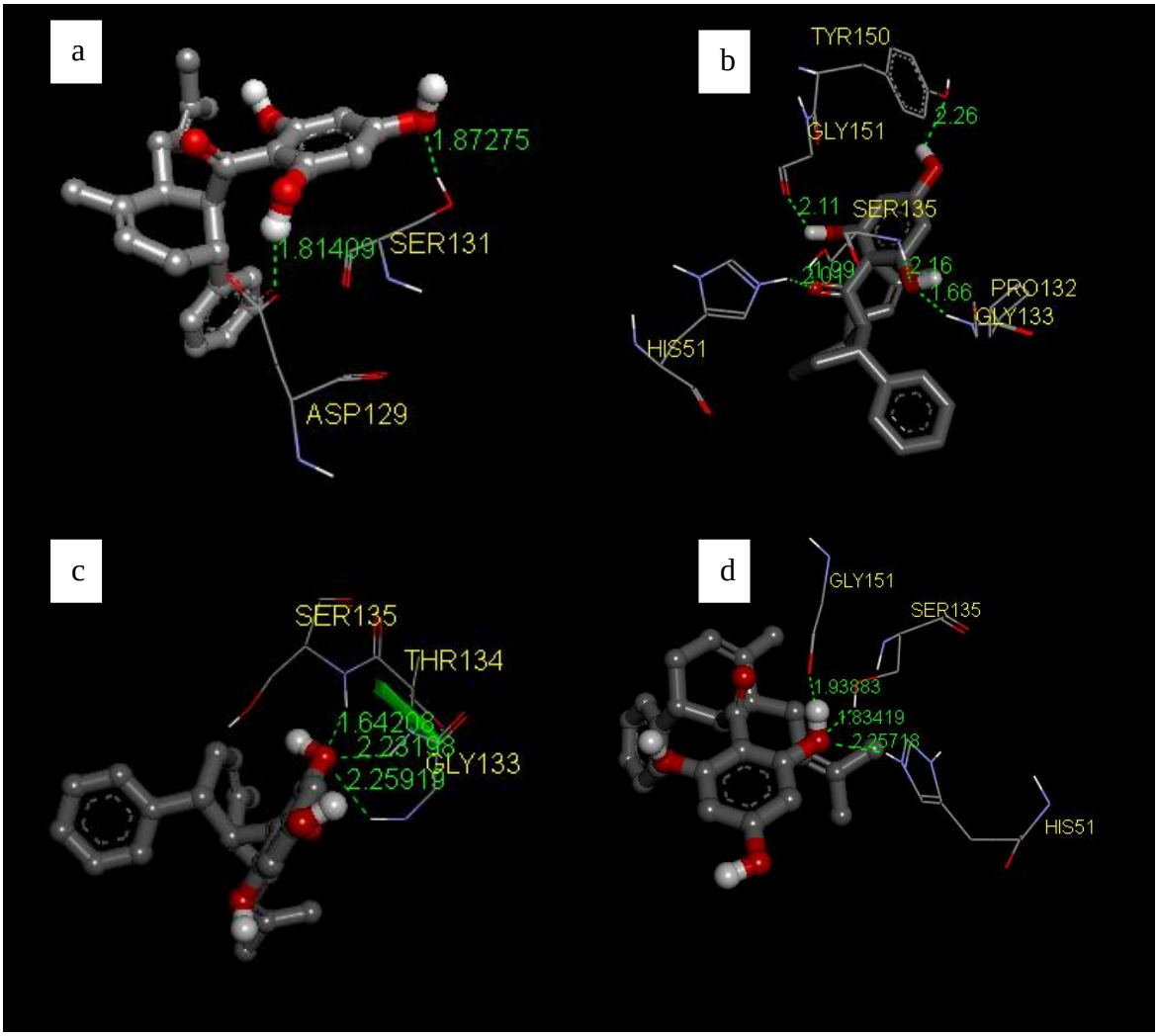

Figure 5: Hydrogen bonding interactions between the 4-hydroxypanduratin A and the DENV NS2B-NS3 proteases using Accerlys Discovery Studio v3.1. Visualiser: (a) 2FOMP7; (b) 3U1J; (c) 3U1I_1; (d) 3U1I_2. The hydrogen bonds (H-bonds) are shown in green and corresponding amino acid residues are labelled in yellow. Atom colours: red is 0, white is H, grey is C and blue is N.

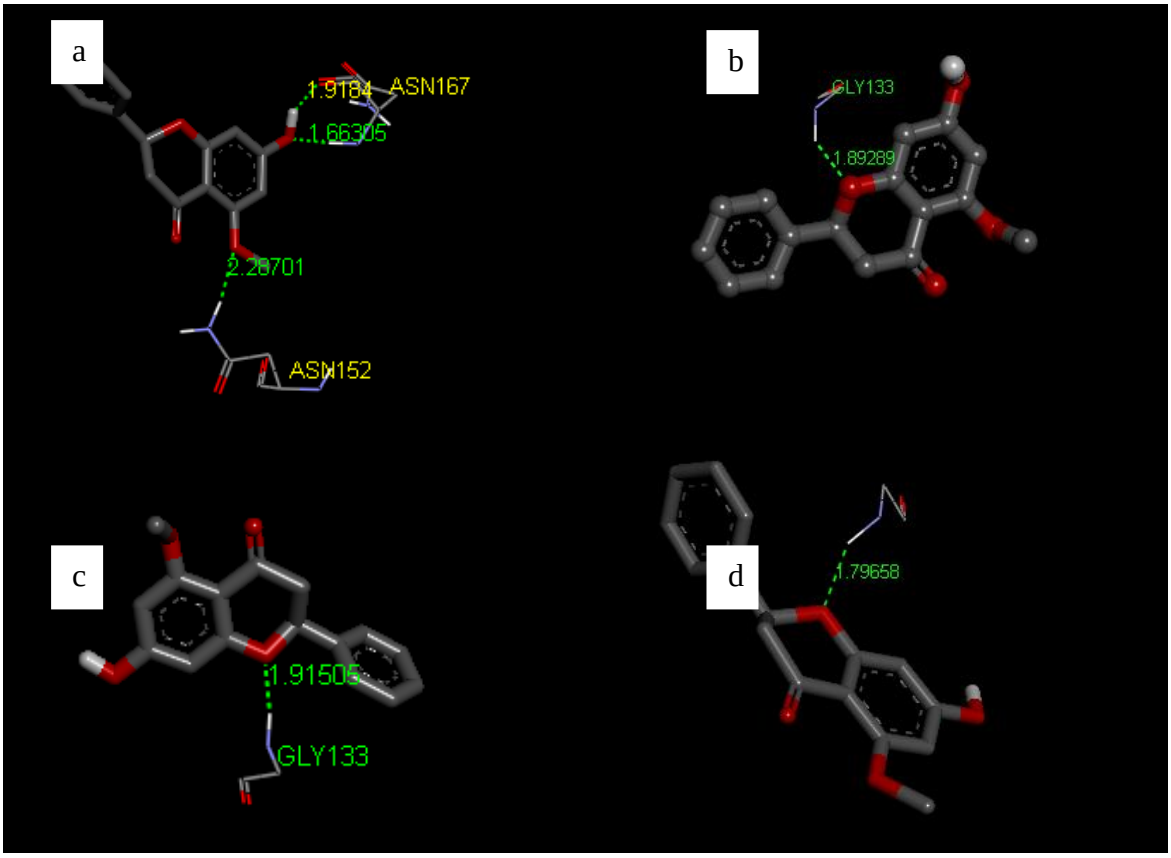

Figure 6: Hydrogen bonding interactions between the alpinetin and the DENV NS2B-NS3 proteases using Accerlys Discovery Studio v3.1. Visualiser: (a) 2FOMP7; (b) 3U1J; (c) 3U1I_1; (d) 3U1I_2. The hydrogen bonds (H-bonds) are shown in green and corresponding amino acid residues are labelled in yellow. Atom colours: red is 0, white is H, grey is C and blue is N.

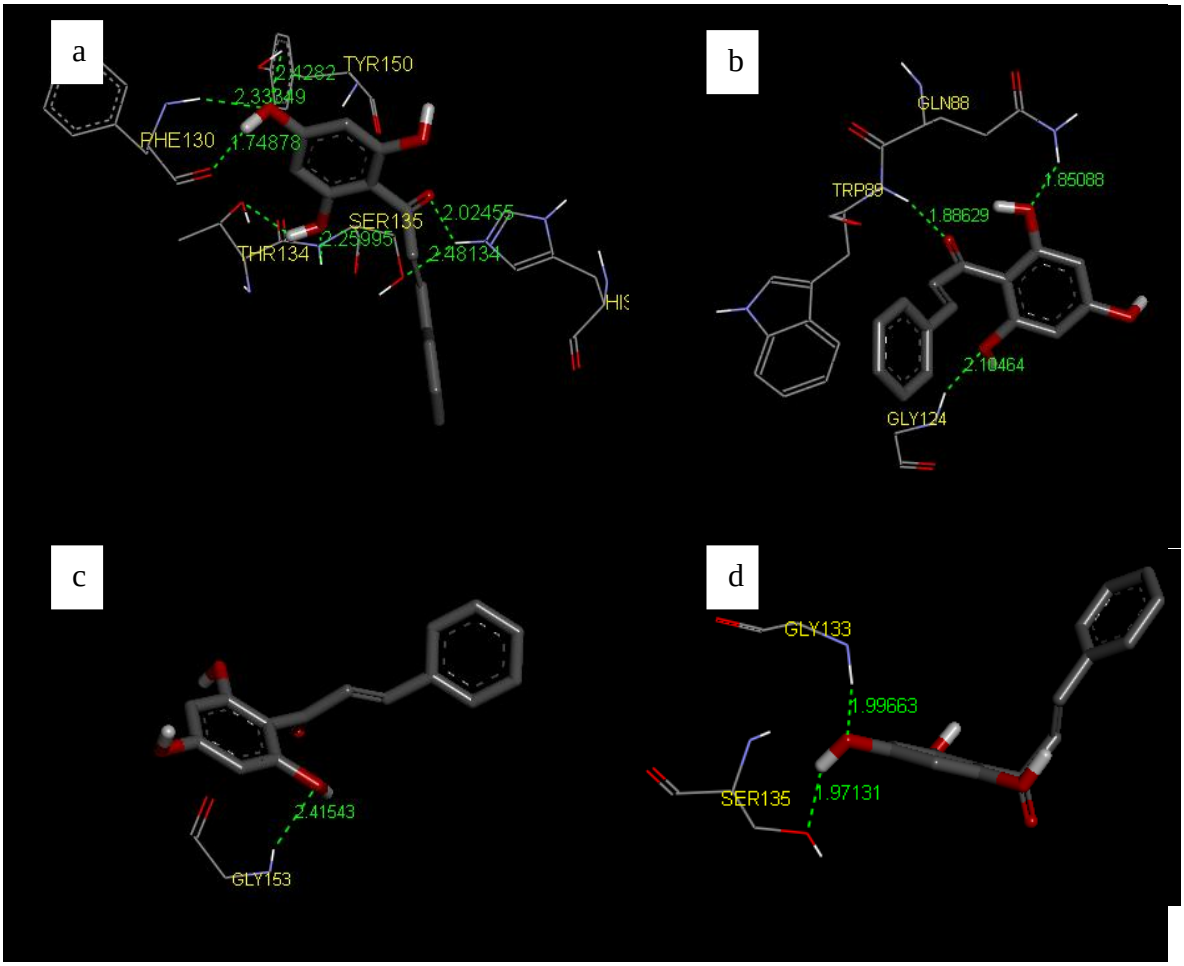

Figure 7: Hydrogen bonding interactions between the pinocembrin and the DENV NS2B-NS3 proteases using Accerlys Discovery Studio v3.1. Visualiser: (a) 2FOMP7; (b) 3U1J; (c) 3U1I_1; (d) 3U1I_2. The hydrogen bonds (H-bonds) are shown in green and corresponding amino acid residues are labelled in yellow. Atom colours: red = 0, white = H, grey = C and blue =N.

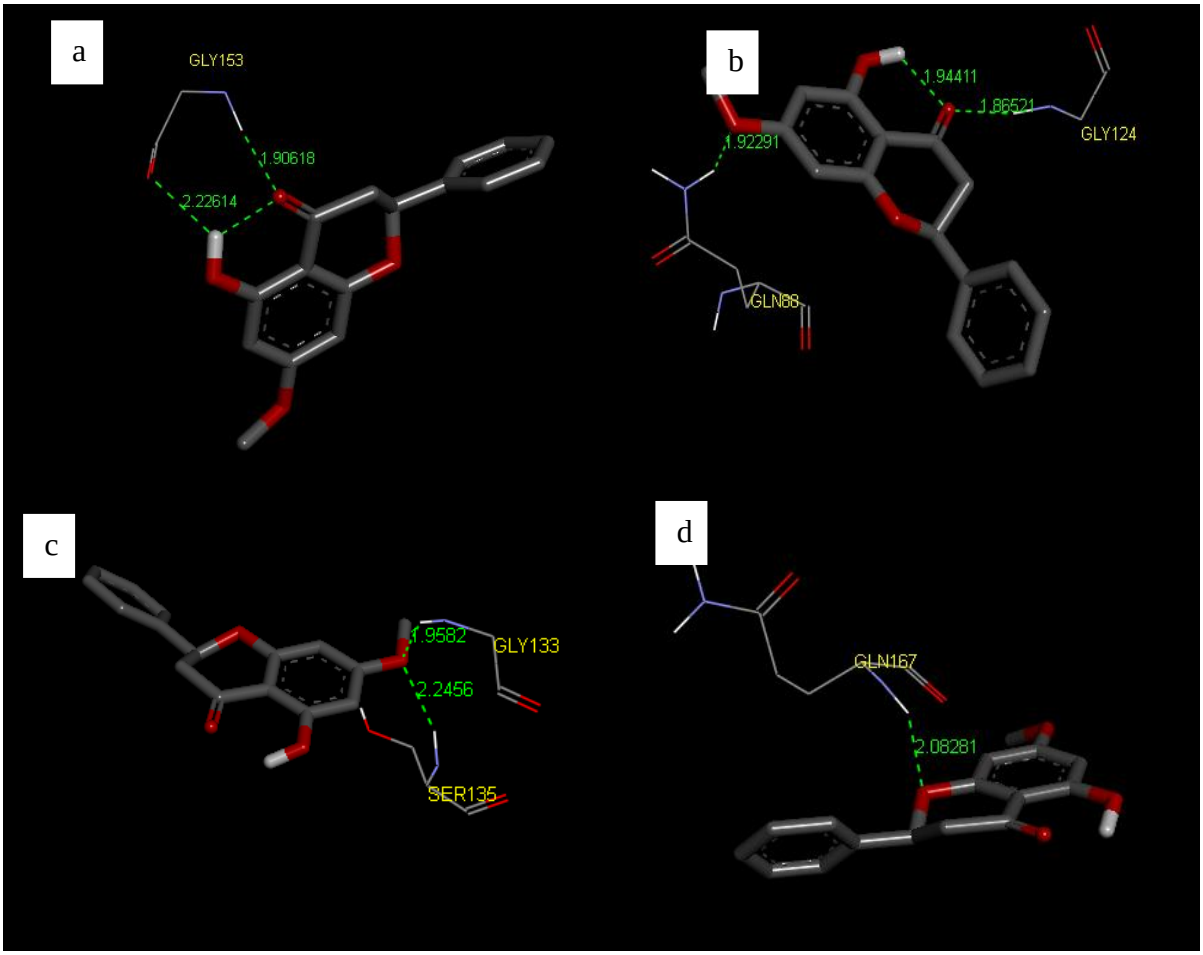

Figure 8: Hydrogen bonding interactions between the pinostrobin and the DENV NS2B-NS3 proteases using Accerlys Discovery Studio v3.1. Visualiser: (a) 2FOMP7; (b) 3U1J; (c) 3U1I_1; (d) 3U1I_2. The hydrogen bonds (H-bonds) are shown in green and corresponding amino acid residues are labelled in yellow. Atom colours: red = 0, white = H, grey = C and blue =N.

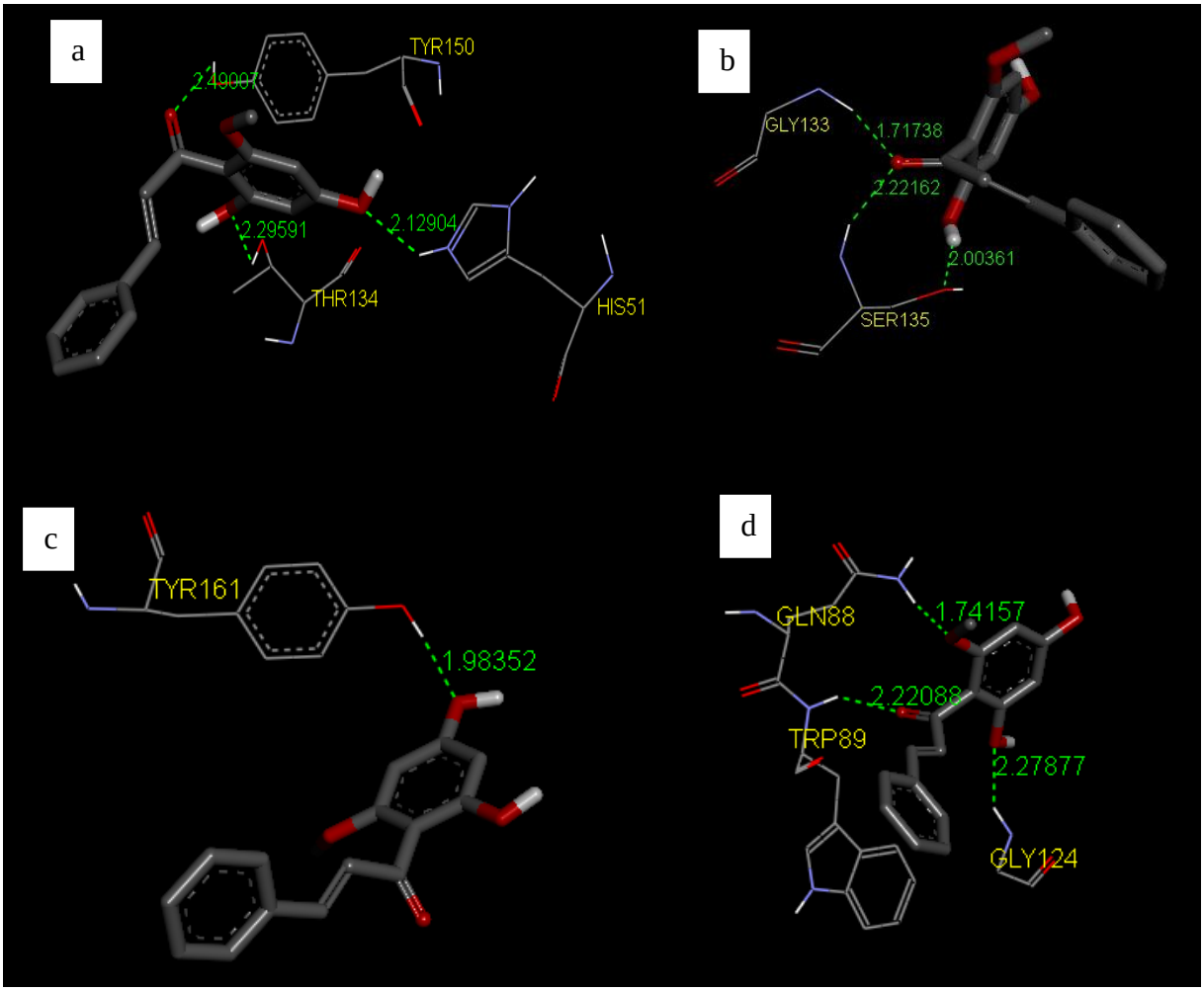

Figure 9: Hydrogen bonding interactions between the cardamonin and the DENV NS2B-NS3 proteases using Accerlys Discovery Studio v3.1. Visualiser: (a) 2FOMP7; (b) 3U1J; (c) 3U1I_1; (d) 3U1I_2. The hydrogen bonds (H-bonds) are shown in green and corresponding amino acid residues are labelled in yellow. Atom colours: red = 0, white = H, grey = C and blue =N.

5.3.2. Hydrophobic interactions

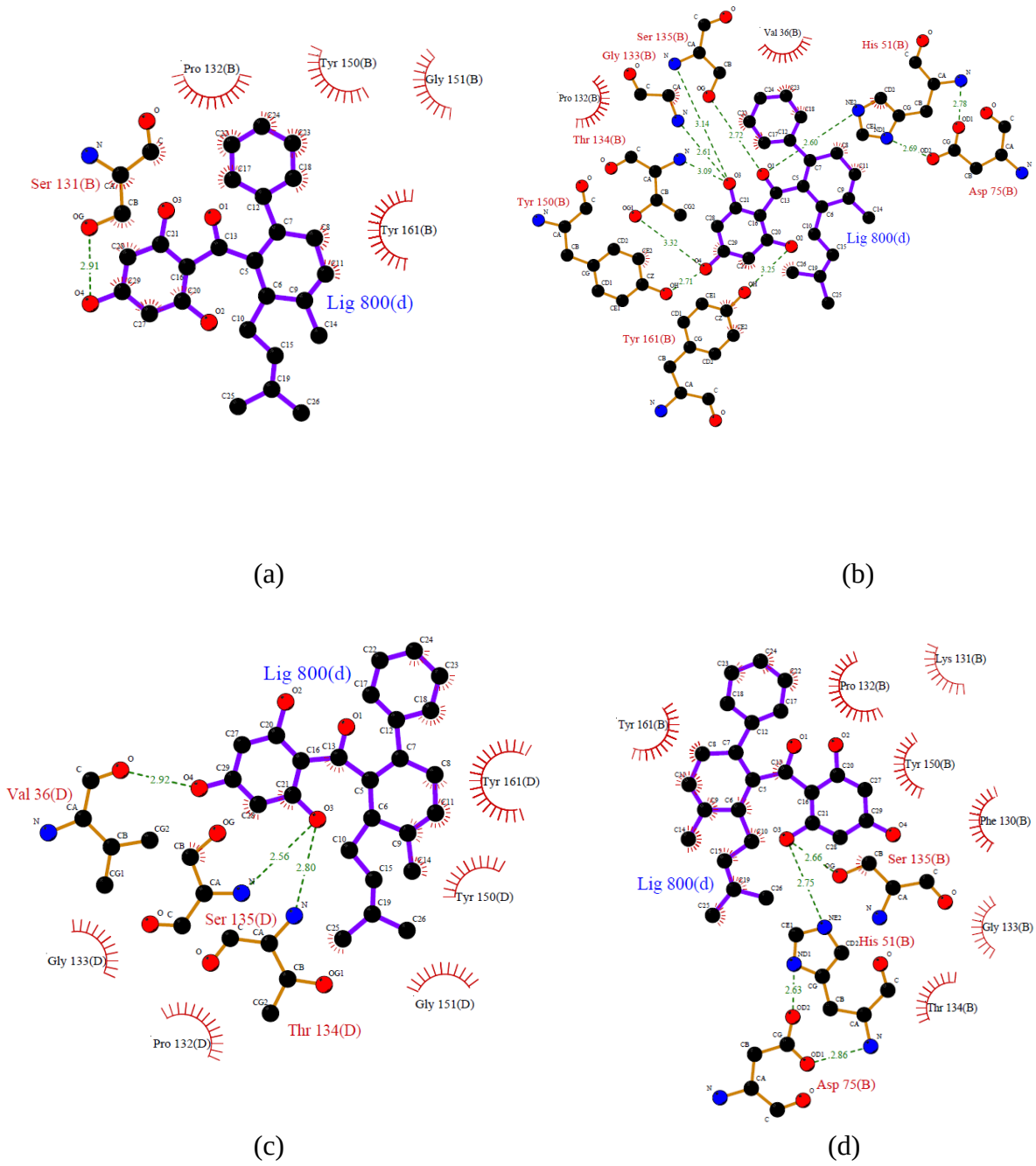

Figure 10: Ligplot 2D representations of the binding modes of 4-hydroxypandurratin A (4-HPA) on (a) 2FOMP7 , (b) 3U1J, (c) 3U1I_1, (d) 3U1I_2, NS2B-NS3 serine proteases. A 2D representation of ligand binding interaction model showing the ligand in purple, residues involved in hydrogen bonding with the ligand in brown with the corresponding hydrogen bond in dotted green line and residues involved in hydrophobic interactions with red spikes.

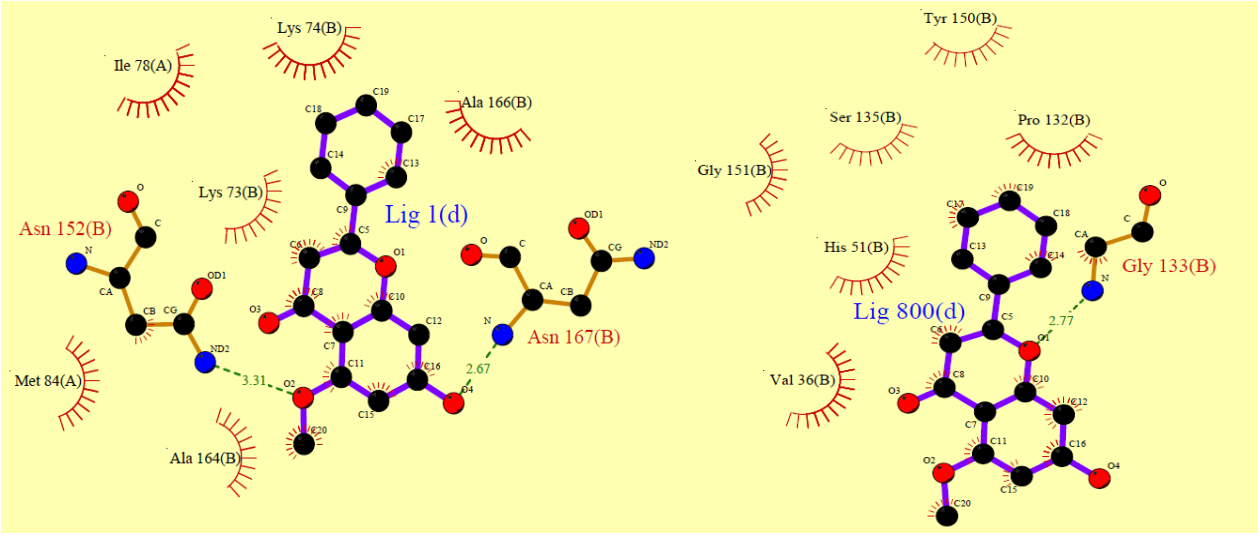

(a) (b)

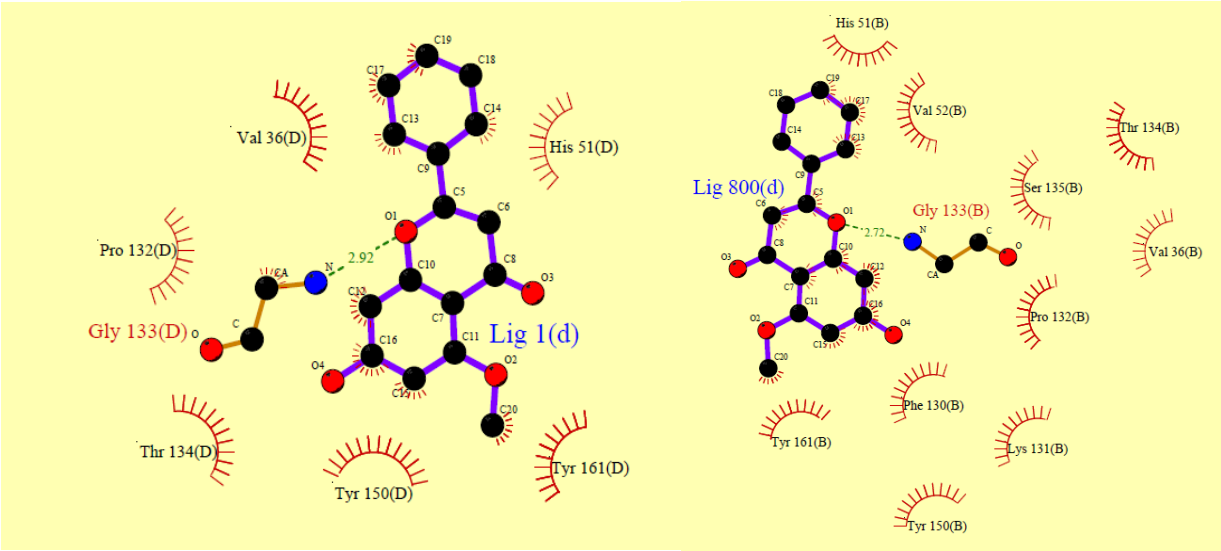

(c) (d)

Figure 11: Ligplot 2D representations of the binding modes of alpinetin on (a) 2FOMP7 , (b) 3U1J, (c) 3U1I_1, (d) 3U1I_2, NS2B-NS3 serine proteases A 2D representation of ligand binding interaction model showing the ligand in purple, residues involved in hydrogen bonding with the ligand in brown with the corresponding hydrogen bond in dotted green line and residues involved in hydrophobic interactions with red spikes.

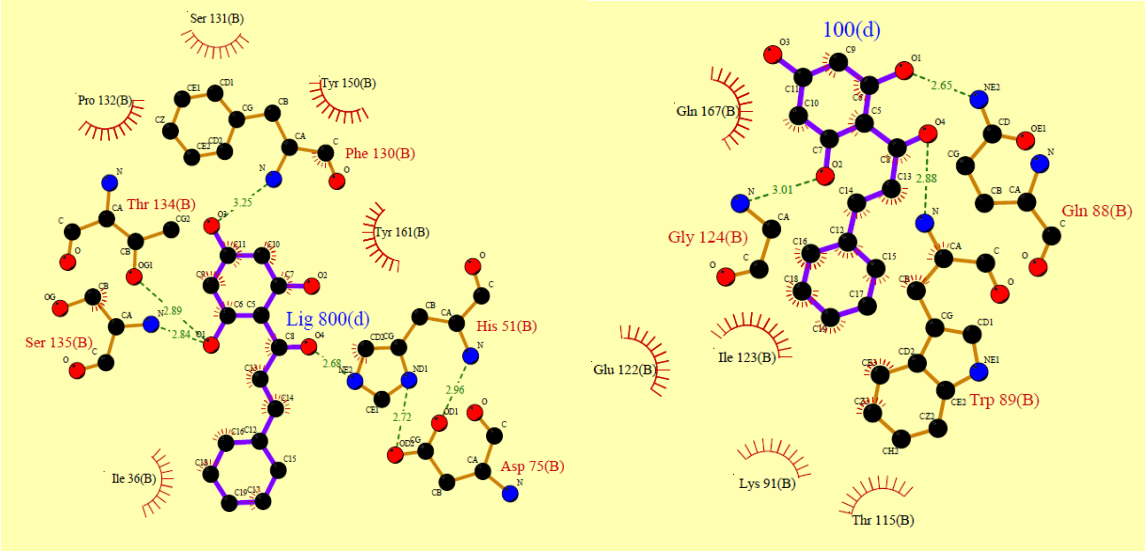

(a) (b)

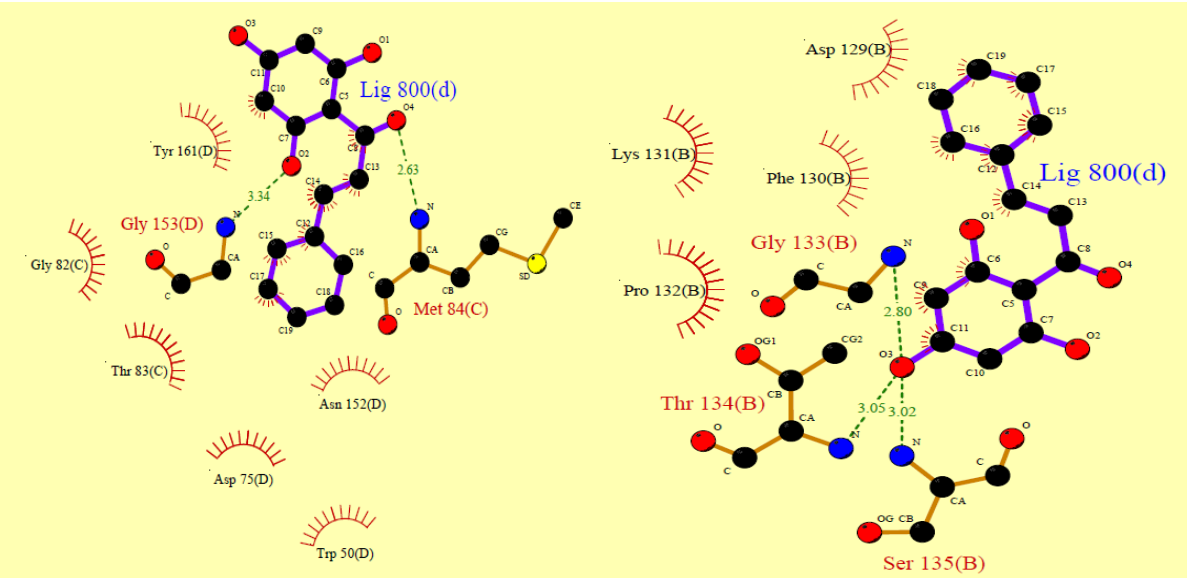

(c) (d)

Figure 12: Ligplot 2D representations of the binding modes of pinocembrin on (a) 2FOMP7 , (b) 3U1J, (c) 3U1I_1, (d) 3U1I_2, NS2B-NS3 serine proteases. A 2D representation of ligand binding interaction model showing the ligand in purple, residues involved in hydrogen bonding with the ligand in brown with the corresponding hydrogen bond in dotted green line and residues involved in hydrophobic interactions with red spikes.

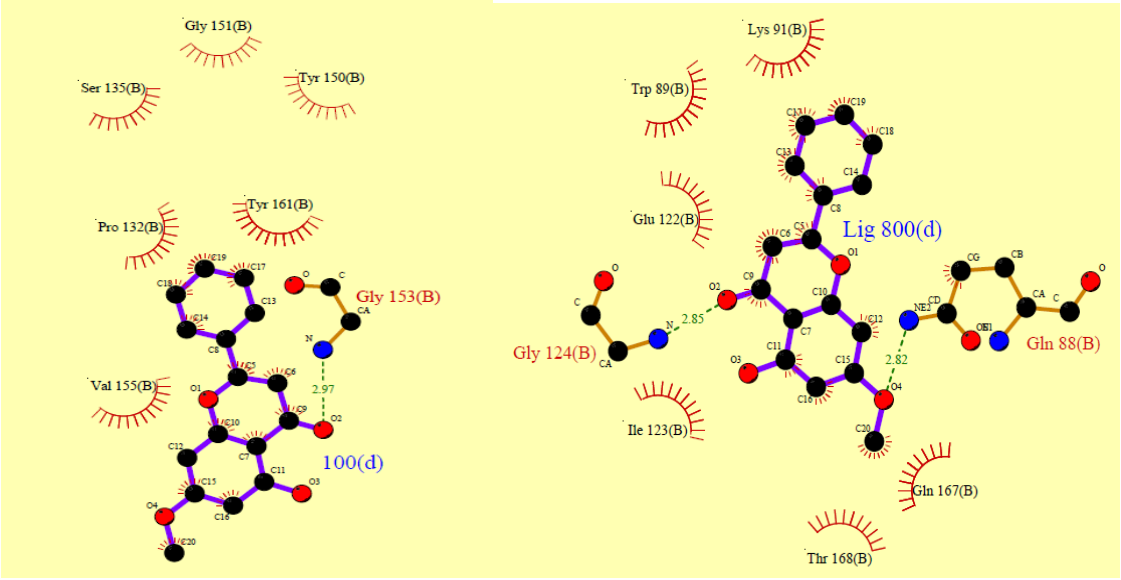

(a) (b)

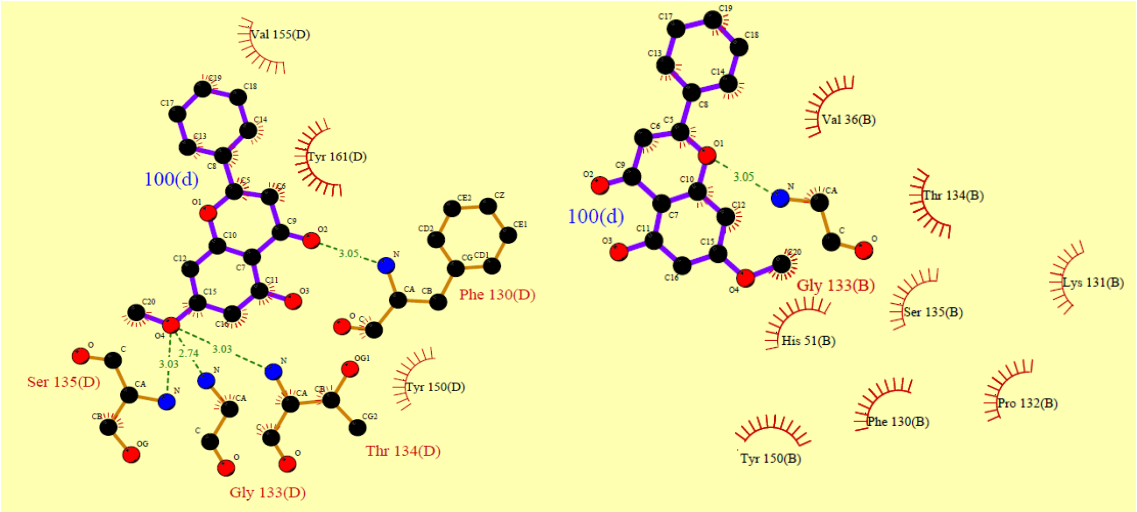

(c) (d)

Figure13: Ligplot 2D representations of the binding modes of pinostrobin on (a) 2FOMP7 , (b) 3U1J, (c) 3U1I_1, (d) 3U1I_2, NS2B-NS3 serine proteases. A 2D representation of ligand binding interaction model showing the ligand in purple, residues involved in hydrogen bonding with the ligand in brown with the corresponding hydrogen bond in dotted green line and residues involved in hydrophobic interactions with red spikes.

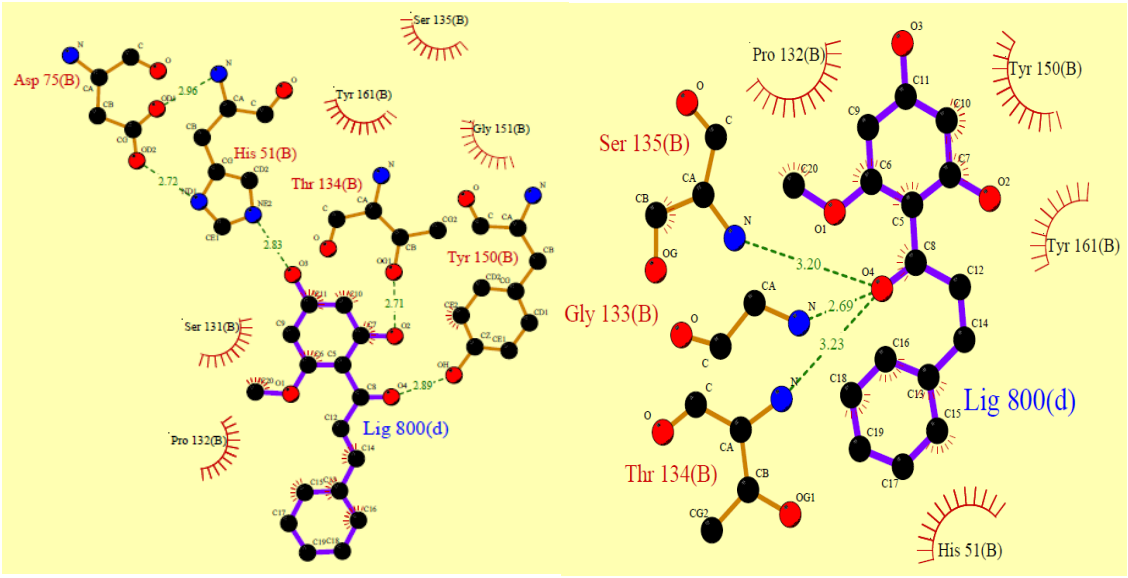

(a) (b)

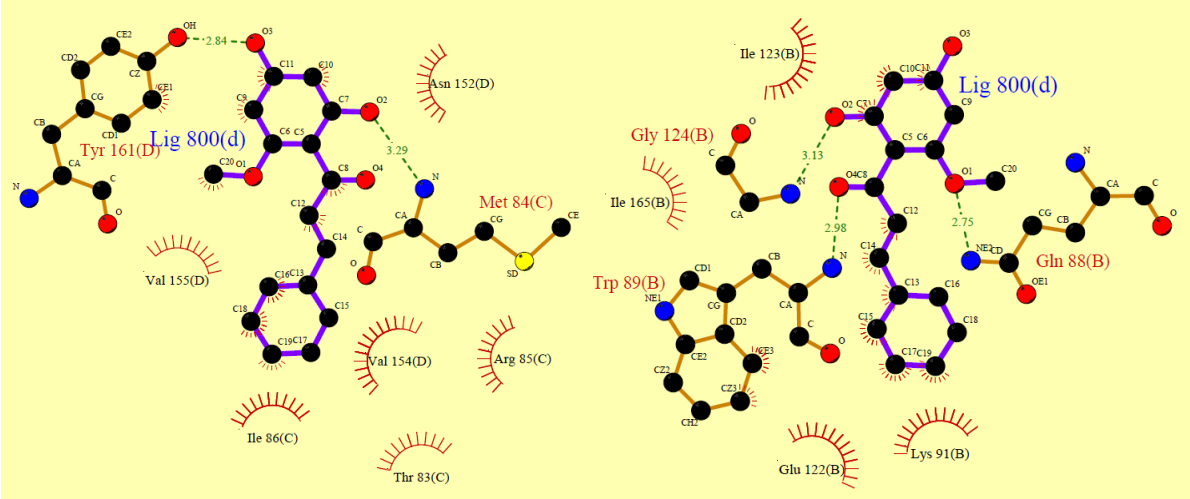

(c) (d)

Figure 14: Ligplot 2D representations of the binding modes of cardamonin on (a) 2FOMP7 , (b) 3U1J, (c) 3U1I_1, (d) 3U1I_2, NS2B-NS3 serine proteases. A 2D representation of ligand binding interaction model showing the ligand in purple, residues involved in hydrogen bonding with the ligand in brown with the corresponding hydrogen bond in dotted green line and residues involved in hydrophobic interactions with red spikes.

5.3.3. van der Waals interactions

Accerlys Discovery Visualiser 3.1 Client was used to produce the van der Waals interactions for the docked ligand-protease complex. Figure 15 obtained from Accerlys Discovery Studio 3.1 Visualiser Help Manual shows the key which details the elements interaction properties. Figure 16 - 20 shows the van der Waals interactions residues which are represented by green circles.

Element	Description
LEU A:100	Residues involved in hydrogen-bond, charge or polar interactions are represented by pink circles.
LEU A:100	Residues involved in van der Waals interactions are represented by green circles.
HOH A:100	Water molecules are represented by aquamarine circles.
ZN A:100	Metal atoms are represented by gray circles.
HIS A:100	Covalently bonded residues are represented by magenta-colored circles.
HIS A:100	The solvent accessible surface of an interacting residue is represented by a blue halo around the residue. The diameter of the circle is proportional to the solvent accessible surface.
O	The solvent accessible surface of an atom is represented by a blue halo around the atom. The diameter of the circle is proportional to the solvent accessible surface.
	Hydrogen-bond interactions with non-amino acid residues are represented by a black dashed line arrow directed towards the electron donor.
	Hydrogen-bond interactions with amino acid main chains are represented by a green dashed arrow directed towards the electron donor.
	Hydrogen-bond interactions with amino acid side-chains are represented by a blue dashed arrow directed towards the electron donor.
	Charge interactions are represented by a pink dashed arrow with heads on both sides.
π σ	Pi interactions are represented by an orange line with symbols indicating the interaction.

Figure 15: Accerlys Discovery Studio Visualiser 3.1 Client 2D diagram style key definitions for the various elements in the 2D Window when displayed using the default colours and graphics (Discovery Studio 3.1. Help manual).

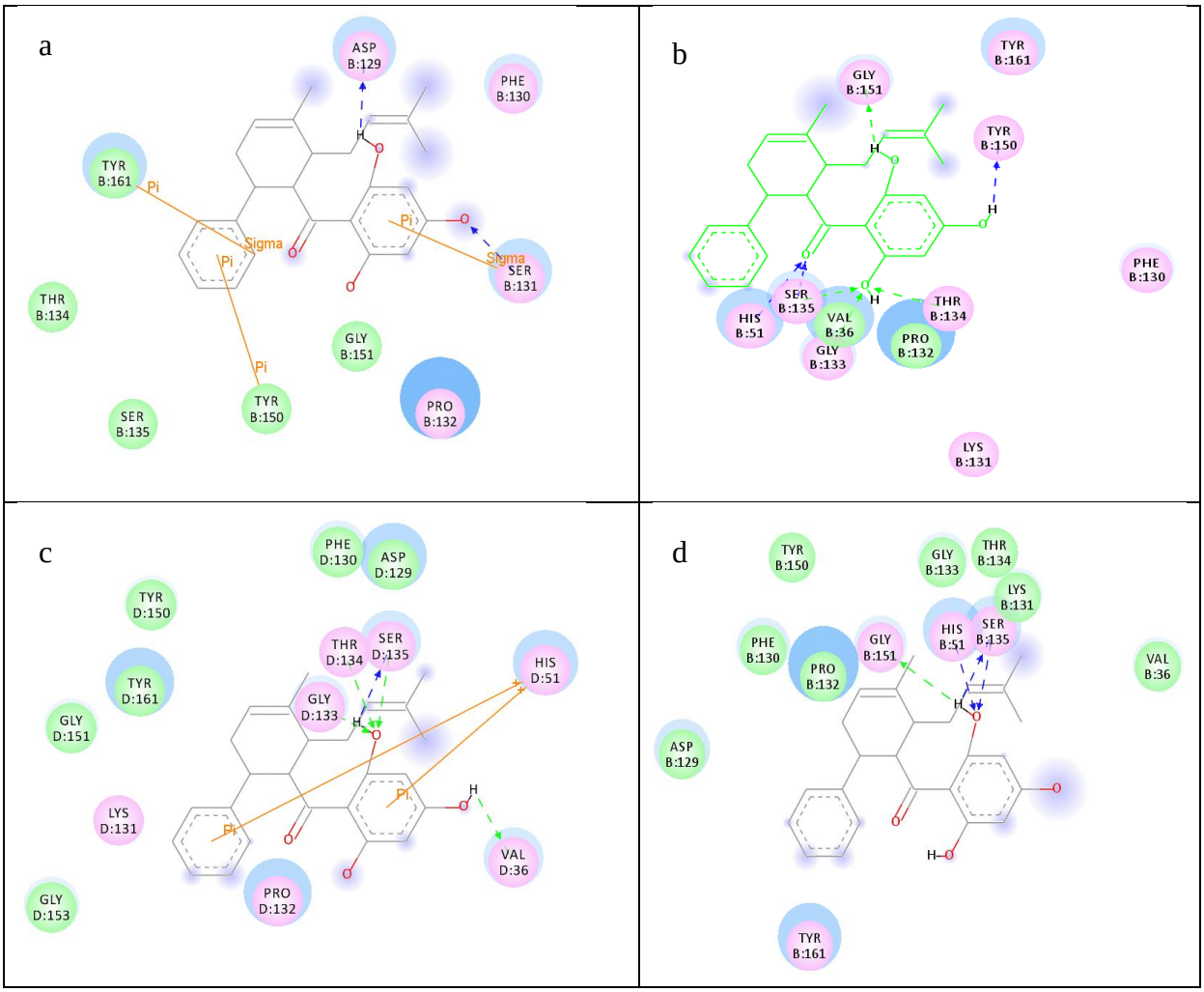

Figure 16: Accerlys Discovery Studio Visualiser 2D representation of binding interaction of (a) DEN2 2FOMP7 homology model and 4-hydroxypanduratin A complex, (b) DEN3 3U1J and 4-hydroxypanduratin A complex, (c) DEN3 3U1I_I and 4-hydroxypanduratin A complex and (d) DEN3 3U1I_2 and 4-hydroxypanduratin A complex.

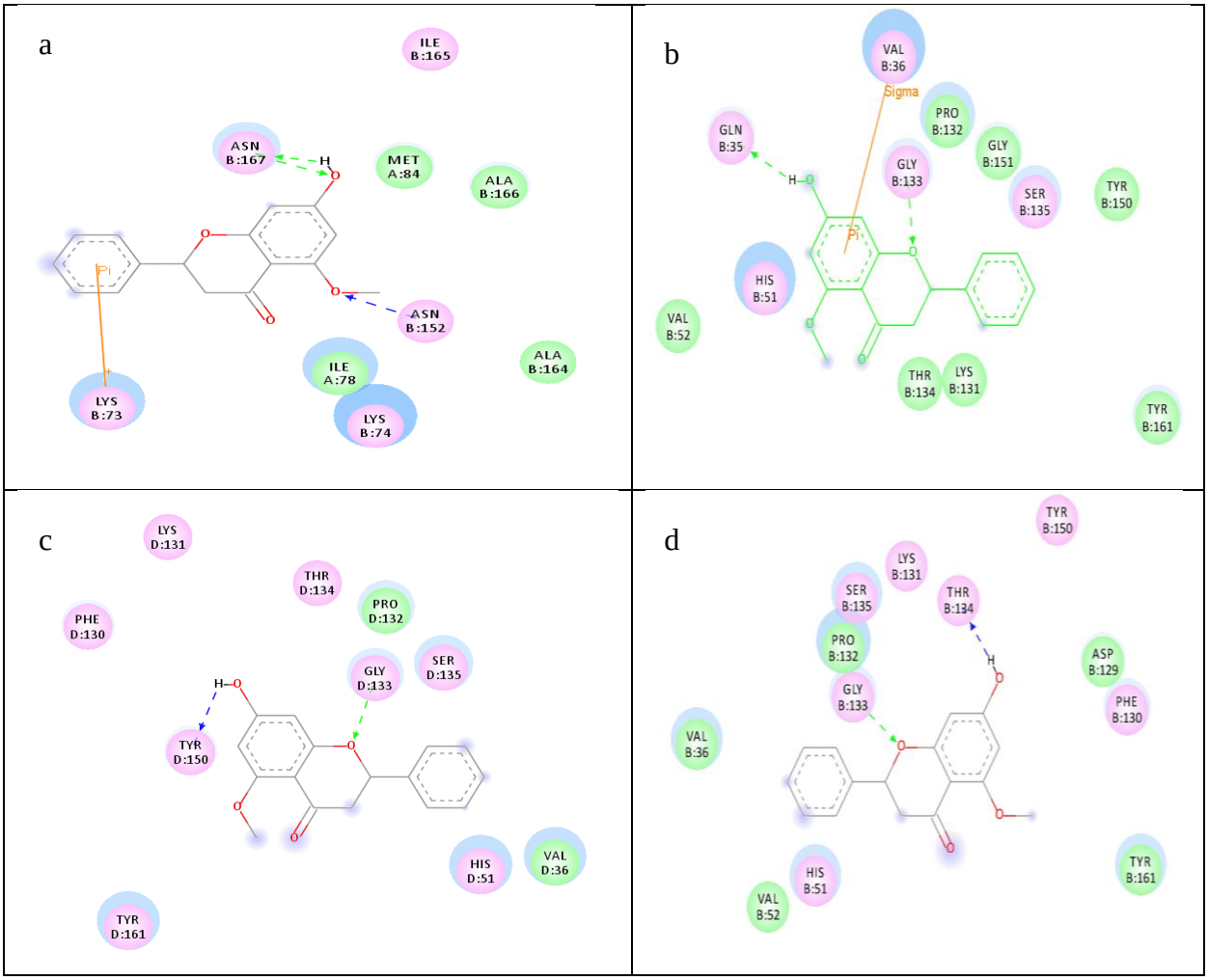

Figure 17: Accerlys Discovery Studio Visualiser 2D representation of binding interaction of (a) DEN2 2FOMP7 homology model and alpinetin complex, (b) DEN3 3U1J and alpinetin complex, (c) DEN3 3U1I_I and alpinetin complex and (d) DEN3 3U1I_2 and alpinetin complex.

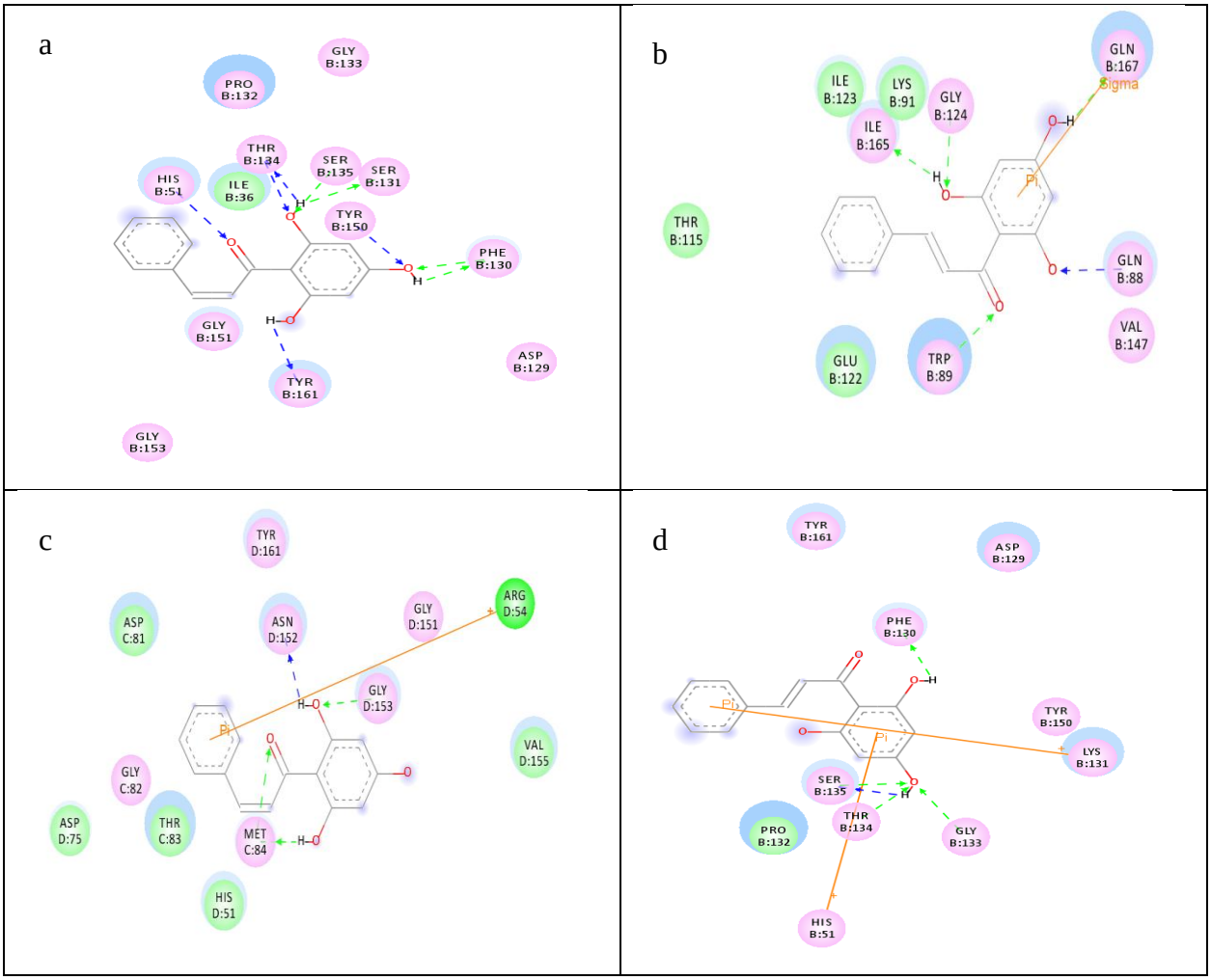

Figure 18: Accerlys Discovery Studio Visualiser 2D representation of binding interaction of (a) DEN2 2FOMP7 homology model and pinocembrin complex, (b) DEN3 3U1J and pinocembrin complex, (c) DEN3 3U1I_I and pinocembrin complex and (d) DEN3 3U1I_2 and pinocembrin complex.

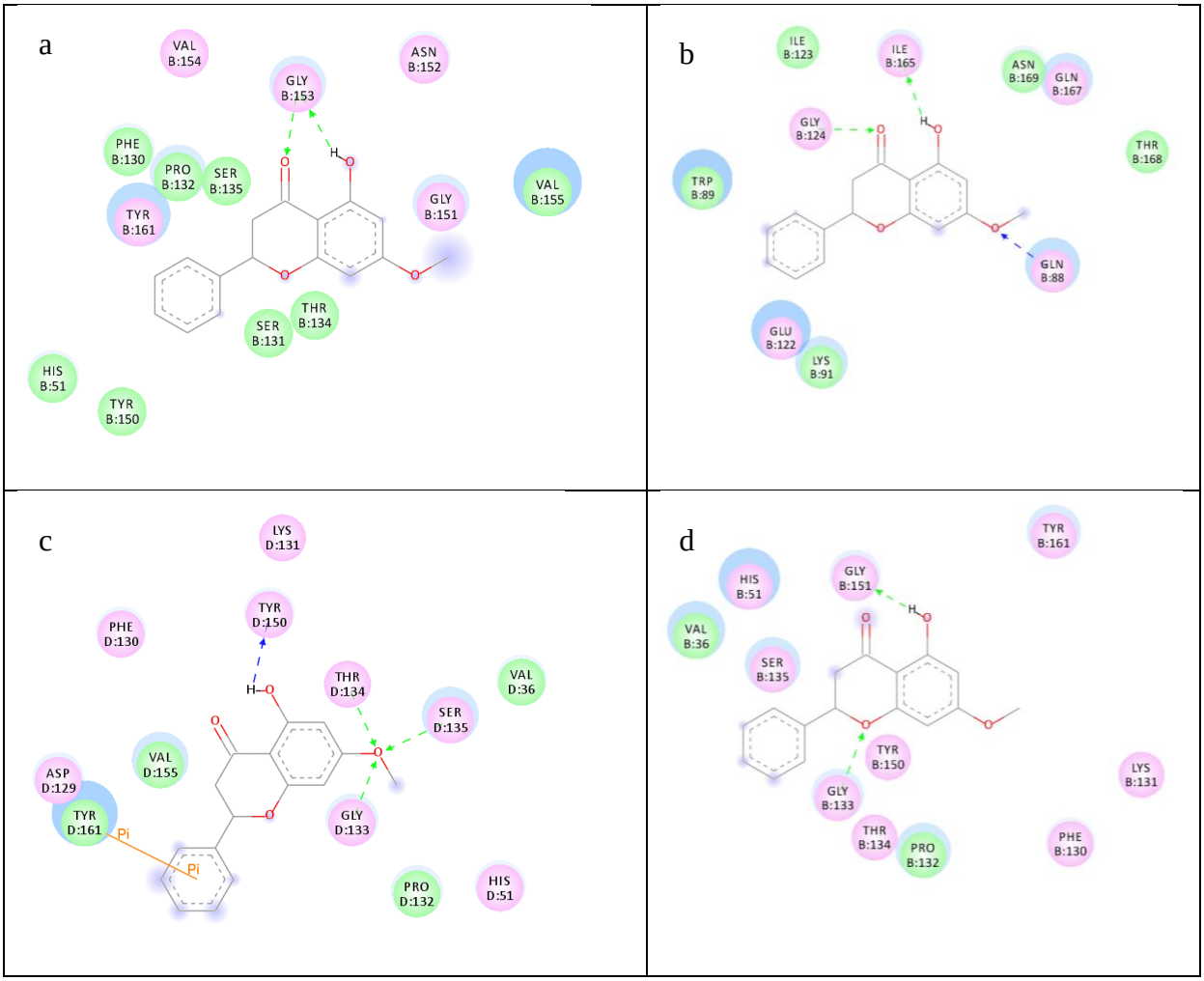

Figure 19: Accerlys Discovery Studio Visualiser 2D representation of binding interaction of (a) DEN2 2FOMP7 homology model and pinostrobin complex, (b) DEN3 3U1J and pinostrobin complex, (c) DEN3 3U1I_I and pinostrobin complex and (d) DEN3 3U1I_2 and pinostrobin complex.

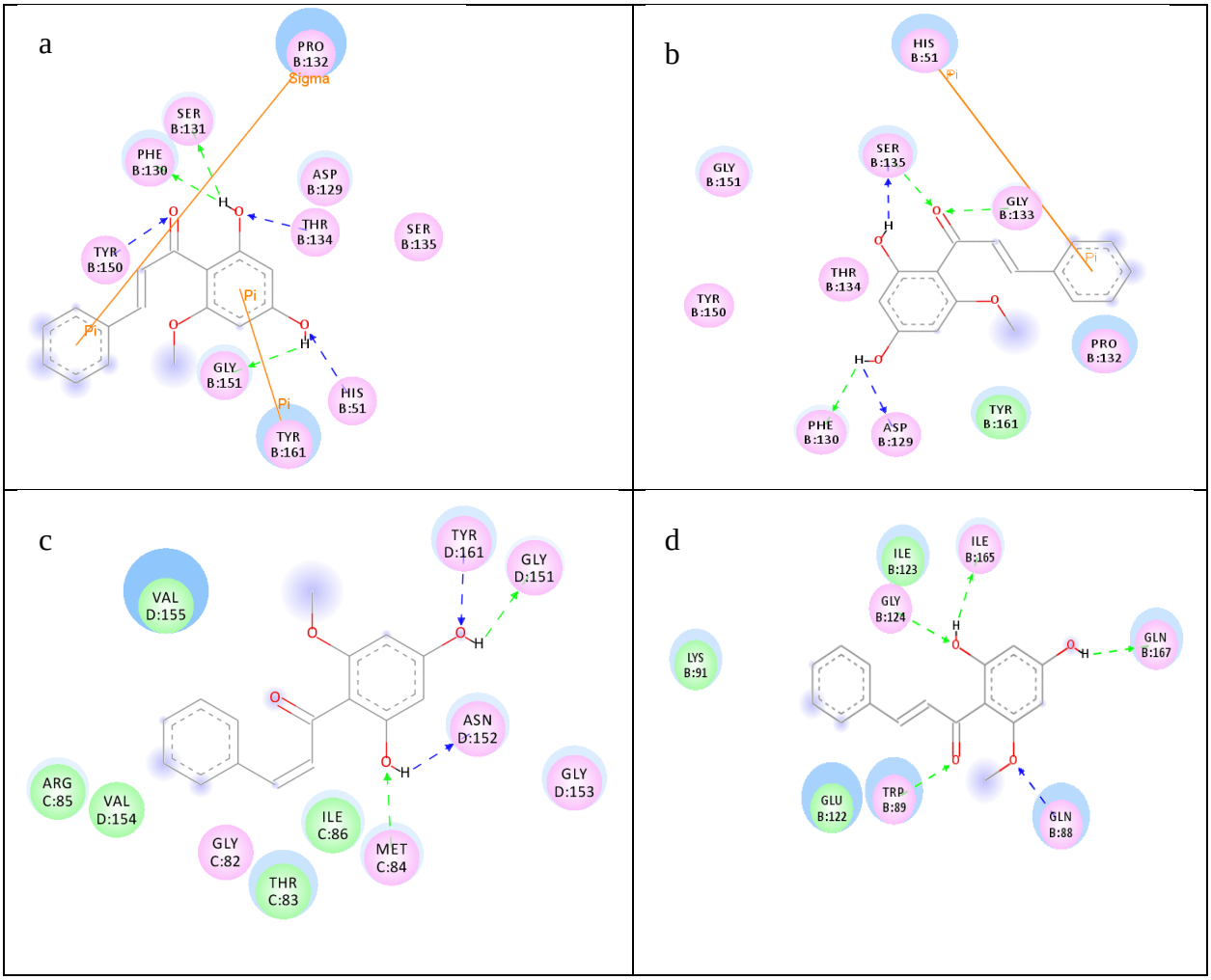

Figure 20: Accerlys Discovery Studio Visualiser 2D representation of binding interaction of (a) DEN2 2FOMP7 homology model and cardamonin complex, (b) DEN3 3U1J and cardamonin complex, (c) DEN3 3U1I_I and cardamonin complex and (d) DEN3 3U1I_2 and cardamonin complex.

6.0. DISCUSSIONS

6.1. Competitive inhibitor

Structural alignment of the DEN2 2FOMP7 homology model and DEN3 protease crystal structures shows that the conserved regions are identical. Thus, comparison of the ligand binding interactions could help to suggest structural optimisation of the ligand for a broad range drug development. Higher specificity towards the Dengue virus proteases could also help reduce interaction with the host proteases. Competitive inhibitor would be able to bind to the active site of the protease and render it inactive for the proteolytic activity of the proteases in processing the RNA genome of the viral replication. The 4-hydroxypanduration A has been reported as an effective competitive inhibitor for the DEN2 protease (Lee et al., 2007). Figure 5 shows the binding mode of 4-hydroxypanduratin A onto DEN2 NS2B-NS3 2FOMP7 homology model, DEN3 NS2B-NS3 3U1J, 3U1I_1 and 3U1I_2 structure. For 2FOMP7, the residue Ser131 forms hydrogen bond with the bond length of 2.91 Å (Figure 5a). Pro132, Tyr150, Gly151 and Tyr161 amino acid residues are involved in hydrophobic interactions with the 4-hydroxypanduratin A (Figure 10a).

Meanwhile, DEN3 NS2B-NS3 3U1J structure (Figure 5b) forms H-bond with His51, Ser135, Gly133, Thr134, Tyr150 and Tyr161 residues. Hydrophobic interactions are observed at Val36 and Pro132 (Figure 10b). H-bond between the Asp75 and His51 residues was observed. The hydrogen bonds is observed to be centered towards the benzyl ring of the 4-hydroxypanduratin A structure. Figure 10c shows the Ligplot 2D output for DEN3 NS2B-NS3 3U1I_1 structure docked with 4-hydroxypanduratin A. Residues Ser135 and Val36 forms H-bond with the ligand. Hydrophobic interactions were observed at residues Tyr161, Tyr150, Gly151, Pro132, and Gly133. DEN3 NS2B-NS3 3U1_2 structure shows that the active site residues His51, Ser135 Gly151 forms H-

bond with 4-hydroxypanduratin A. Residues Tyr161, Pro132, Tyr150, Phe130, Lys131, Gly133 and Thr134 are involved in hydrophobic interactions.

Previous reports suggests that 4-hydroxypanduratin A involved in H-bond with Asp75, Ser135 and Gly151. The hydroxyl group of 4-hydoxypanduratin A binding to the Asp75 residue has shown to be contributing to the lower estimated inhibitory constant (Lee et al., 2007). It was observed with a decrease bond distances. Increase in bond distance decreases the inhibitory activity. Ser135 is denoted as the important residue to identify and select a hit of the ligands by Valle et al. (1998) because the authors found that the substitution of the catalytic serine by alanine resulted in an enzymatically inactive NS3 protein.

Ligand interacting with Pro132 has been reported to obstruct the interaction of the protease Ser135 with the ligand (Tomlinson et. al., 2011). Pro132 in both DEN2 2FOMP7 and DEN3 proteases crystal structures was found to be interacting with the competitive ligand by forming hydrophobic interactions. The residue His51 was found to form H-bond with the 4-hydroxypanduratin A on the DEN3 crystal structures and does not involve in van Der Waals interaction as compared to the reported DEN2 protease by Lee et. al., (2007). Residue His51 is more involved in H-bond in this study for all the DEN3 structures and was not predicted to be interacting with the DEN2 NS2B-NS3 2FOMP7 homology model.

6.2. Non-competitive inhibitors

The degree of estimated inhibition value for the alpinetin, pinocembrin, pinostrobin and cardamonin shows higher potency on DEN3 3U1J protease compared to the DEN 2FOMP7 homology model, 3U1I_1 and 3U1I_2 proteases. Binding of non-competitive inhibitors shows the alternative binding pocket away from the catalytic triad. Figure 7a shows Asn162 and Asn167 forms H-bond with alpinetin and the surrounding residues that forms hydrophobic interactions are Ile 78, Lys74, Ala166, Ala164 and Met84. However, 3U1J structure forms H-bond with alpinetin at Gly133 and His51, Ser135, Val36, Gly151, Pro132 and Tyr150 amino acid residues forms hydrophobic interactions. Meanwhile, the DEN3 3U1I_1 structure shows that the Gly133 residue formed H-bond with alpinetin. His51, Tyr161, Tyr150, Thr134, Pro132 and Val36 form hydrophobic binding interactions with alpinetin. DEN3 NS2B-NS3 3U1I_2 structure also interacts with alpinetin and forms hydrogen bond at Gly133. This show Gly133 is an important residue for the binding of alpinetin in DEN3 NS2N-NS3 protease.

Pinocembrin was reported to be forming hydrogen bond with Leu149 and Asn152 (Othman et al., 2008). In addition, pinocembrin formed an additional H-bond with Val147 and Ile165 with DEN2 NS2B-NS3. In this study however, it is observed that H-bonds did not involve Leu149 and Asn 152. The observed interaction of van der Waals for 2FOMP7 was with Ile36. The residues Lys91, Thr115, Glu122, Ile123 interacted with DEN3 3U1J protease. DEN3 3U1I_1 protease shows van der Waals interaction with His51, Arg54, Asp75, Asp81, Thr83, and Val155. 3U1I_2 protease shows van der Waals interaction with Pro132.

The prediction of pinostrobin binding mode showed 2FOMP7 forms hydrogen bond with Gly153. Hydrophobic interactions are with Pro132, Ser135, Tyr150, Gly151, Val155, Tyr161 residues and van der Waals interaction was shown to be involving the catalytic triad and other additional residues such as His51, Phe130, Pro132, Ser131, Thr134, Ser135, Tyr150, and Val155. Pinostrobin formed H-bond with DEN3 3U1_1 protease at Gly133, Thr134, Ser135, Tyr150. Similar binding modes are observed for the pinocembrin, pinostrobin and cardamonin where Gly133 is involved in hydrogen bond interaction. Cardamonin showed no van der Waals interaction with the DEN2 2FOMP7 homology model but shows hydrophobic interactions with Ser131, Pro132, Ser135, Gly151 and Tyr161.

In this study, it is observed that there were more hydrophobic interactions with the ligands compared to the hydrogen bonding interactions. The intermolecular interaction allows the binding of the ligands with directionality with a lower the free energy of binding. This suggests that this binding affinity of the ligand to the macromolecule could be increased by incorporating these residues at the hydrogen bonding amino acid residues. This can be achieved by manipulating the donors and acceptors of the ligand molecules to complement the macromolecule at the active site core (Davis et. al., 1999; Patil et. al., 2010). The modification improves the stability of the ligand-protein complex and produces a better biological activity to inhibit the functionality of the target protein.

7.0. CONCLUSIONS

This research project is focused on using the computational tools to simulate and predict the most favourable docking models for the DEN2 2FOMP7, DEN3 3U1J, 3U1I_1 and 3U1I_2 structures with regard to the binding interactions. 4-hydroxypanduratin A showed important interactions with the catalytic triad of the proteases. This showed more potency of the estimated inhibitory constant compared to the non-competitive inhibitors. There are several similarities observed in this study compared to reported binding interactions by other researchers for the non-competitive inhibitors. The parameters used for the docking methodology could be further optimised and preparation of the ligand could be subjected to a more stringent structural minimization. Furthermore, it is also recommended to further test these ligands with other docking tools such as GOLD, Glide, DOCK and FlexX to study the reliability and consistency of the results obtained.

Nonetheless, these findings have provide further understanding on the binding interaction of the catalytic triad of the DEN2 NS2B-NS3 serine protease homology model (2FOMP7) and the recently published DEN3 NS2B-NS3 serine protease structures, thus giving input into the mode of action of the catalytic triad which shows lower estimated free binding energy and higher potency of the competitive and non-competitive estimated inhibitory constant. In addition, the future work with in-vitro inhibition studies of these ligands with the DEN3 NS2B-NS3 serine protease will enable a complete comparison between the experimental and in-silico inhibition data analysis of the study on the interactions in detail.

REFERENCES

Alberty, R. A. (2003). Fundamental equation of thermodynamics for protein-ligand binding. Biophysical Chemistry, 104(3), 543-559.

Barril, X., & Morley, S. D. (2005). Unveiling the full potential of flexible receptor docking using multiple crystallographic structures. *Journal of Medicinal Chemistry*, *48*(13), 4432-4443. American Chemical Society.

Bazan, J.F., Fletterick, R.J., (1989). Detection of a trypsin-like serine protease domain in flaviviruses and pestiviruses. Virology, vol. 171, 637-639.

Chandramouli, S., Joseph, J. S., Daudenarde, S., Gatchalian, J., Cornillez-Ty, C., & Kuhn, P. (2010). Serotype-Specific Structural Differences in the Protease-Cofactor Complexes of the Dengue Virus Family. Journal of Virology, 84(6), 3059-3067.

Davis AM, Teague SJ (1999) Hydrogen bonding, Hydrophobic Interactions, and Failure of the Rigid Receptor hypothesis. Angew Chem Int Ed 38: 736–749.

Falgout, B., Pethel, M.; Zhang, Y. M.; Lai, C. J. (1991). Both non-structural proteins NS2B and NS3 are required for the proteolytic processing of dengue virus nonstructural proteins. Journal of Virology. vol.65, 2467–2475.

Huey, R., & Morris, G. M. (2009). Using AutoDock with AutoDockTools : A Tutorial. Search, (August), 1-13. The Scripps Research Insti tute. Retrieved from http://203.200.217.185:8000/bic/molvis/softwares/-UsingAutoDockWithADT.pdf.

Lee, Y. K., Kiat, T. S., Wahab, H. A., Yusof, R., & Rahman, N. A. (2007). Nonsubstrate Based Inhibitors of Dengue Virus Serine Protease: A Molecular Docking Approach to Study Binding Interactions between Protease and Inhibitors. AsiaPacific Journal of Molecular Biology and Biotechnology, vol.15(2), 53-59.

McMichael, A. J. (1998). The original sin of killer T cells. Nature. Retrieved from http://www.ncbi.nlm.nih.gov/pubmed/9697760

Noble, C. G., Cheah, C. S., Chao, A. T., Pei, Y. S. (2012). Ligand-Bound structures of the Dengue Virus Protease reveal the active conformation. Journal of Virology, vol. 86, 1438-1446.

Patil R, Das S, Stanley A, Yadav L, Sudhakar A, (2010) Optimized Hydrophobic Interactions and Hydrogen Bonding at the Target-Ligand Interface Leads the Pathways of Drug-Designing. PLoS ONE 5(8): e12029.

Othman, R., Kiat, T. S., Khalid, N., Yusof, R., Newhouse, E. I., Newhouse, J. S., Alam, M., (2008). Docking of noncompetitive inhibitors into dengue virus type 2 protease: understanding the interactions with allosteric binding sites. Journal of Chemical Information and Modeling, vol.48(8), 1582-1591. American Chemical Society.

Tomlinson, S. M., Watowich, S. J. (2011). Anthracene-based Inhibitors of Dengue Virus NS2B-NS3 Protease. Antiviral Research, vol. 89(2), 127-135.

Wang, Q.-Y., Patel, S. J., Vangrevelinghe, E., Xu, H. Y., Rao, R., Jaber, D., Schul, W., (2009). A Small-Molecule Dengue Virus Entry Inhibitor. Antimicrobial Agents and Chemotherapy, 53(5), 1823-1831. American Society for Microbiology (ASM).

APPENDICES

Appendix 1: Grid parameter file (*.gpf) for 4-hydoxypanduratin A.

```
npts 70 70 70                    # num.grid points in xyz
gridfld 2FOMP7.maps.fld          # grid_data_file
spacing 0.375                    # spacing(A)
receptor_types A C HD N OA SA    # receptor atom types
ligand_types A C HD OA           # ligand atom types
receptor 2FOMP7.pdbqt            # macromolecule
gridcenter 36.461 47.31 2.908    # xyz-coordinates or auto
smooth 0.5                       # store minimum energy w/in rad(A)
map 2FOMP7.A.map                 # atom-specific affinity map
map 2FOMP7.C.map                 # atom-specific affinity map
map 2FOMP7.HD.map                # atom-specific affinity map
map 2FOMP7.OA.map                # atom-specific affinity map
elecmap 2FOMP7.e.map             # electrostatic potential map
dsolvmap 2FOMP7.d.map            # desolvation potential map
dielectric -0.1465               # <0, AD4 distance-dep.diel;>0, constant
```

Appendix 2: Docking parameter file (*.dpf) for 4-hydroxypanduratin A.

```
autodock_parameter_version 4.2      # used by autodock to validate parameter set
outlev 1                            # diagnostic output level
intelec                             # calculate internal electrostatics
seed pid time                       # seeds for random generator
ligand_types A C HD OA              # atoms types in ligand
fld 2FOMP7.maps.fld                 # grid_data_file
map 2FOMP7.A.map                    # atom-specific affinity map
map 2FOMP7.C.map                    # atom-specific affinity map
map 2FOMP7.HD.map                   # atom-specific affinity map
map 2FOMP7.OA.map                   # atom-specific affinity map
elecmap 2FOMP7.e.map                # electrostatics map
desolvmap 2FOMP7.d.map              # desolvation map
move 4_hydroxypanduratin_A.pdbqt    # small molecule
about -0.3409 0.0732 -0.034         # small molecule center
tran0 random                        # initial coordinates/A or random
axisangle0 random                   # initial orientation
dihe0 random                        # initial dihedrals (relative) or random
tstep 2.0                           # translation step/A
qstep 50.0                          # quaternion step/deg
dstep 50.0                          # torsion step/deg
torsdof 8                           # torsional degrees of freedom
rmstol 2.0                          # cluster_tolerance/A
extnrg 1000.0                       # external grid energy
e0max 0.0 10000                     # max initial energy; max number of retries
ga_pop_size 150                     # number of individuals in population
ga_num_evals 2500000                # maximum number of energy evaluations
ga_num_generations 27000            # maximum number of generations
ga_elitism 1                        # number of top individuals to survive to next generation
ga_mutation_rate 0.02               # rate of gene mutation
ga_crossover_rate 0.8               # rate of crossover
ga_window_size 10                   #
ga_cauchy_alpha 0.0                 # Alpha parameter of Cauchy distribution
ga_cauchy_beta 1.0                  # Beta parameter Cauchy distribution
set_ga                              # set the above parameters for GA or LGA
sw_max_its 300                      # iterations of Solis & Wets local search
sw_max_succ 4                       # consecutive successes before changing rho
sw_max_fail 4                       # consecutive failures before changing rho
sw_rho 1.0                          # size of local search space to sample
sw_lb_rho 0.01                      # lower bound on rho
ls_search_freq 0.06                 # probability of performing local search on individual
set_psw1                            # set the above pseudo-Solis & Wets parameters
unbound_model bound                 # state of unbound ligand
ga_run 100                          # do this many hybrid GA-LS runs
analysis                            # perform a ranked cluster analysis
```

Appendix 3: The coordinate of the chosen docked conformer of 4-hydroxypanduratin A obtained from the docking log file (*.dlg).

```
MODEL       21
USER    Run = 21
USER    Cluster Rank = 5
USER    Number of conformations in this cluster = 60
USER
USER    RMSD from reference structure       = 48.909 A
USER
USER    Estimated Free Energy of Binding    =   -3.72 kcal/mol  [=(1)+(2)+(3)-(4)]
USER    Estimated Inhibition Constant, Ki   =    1.87 mM (millimolar)  [Temperature =
298.15 K]
USER
USER    (1) Final Intermolecular Energy     =   -6.11 kcal/mol
USER        vdW + Hbond + desolv Energy     =   -5.82 kcal/mol
USER        Electrostatic Energy            =   -0.29 kcal/mol
USER    (2) Final Total Internal Energy     =   -1.50 kcal/mol
USER    (3) Torsional Free Energy           =   +2.39 kcal/mol
USER    (4) Unbound System's Energy  [=(2)] =   -1.50 kcal/mol
USER
USER
USER
USER    DPF = 2FOMP7-4HPA.dpf
USER    NEWDPF move       4_hydroxypanduratin_A.pdbqt
USER    NEWDPF about      -0.340900 0.073200 -0.034000
USER    NEWDPF tran0      30.935080 40.345343 -4.503809
USER    NEWDPF axisangle0          0.454658 -0.198425 0.868282 -163.063125
USER    NEWDPF quaternion0         0.449701 -0.196262 0.858815 -0.147265
USER    NEWDPF dihe0      -112.38 -75.86 58.01 46.62 -80.84 -28.92 -20.16 -1.41
USER
USER                          x       y       z    vdW   Elec       q     RMS
ATOM      1  O1  SUB dUNIT     29.128  39.884  -5.575 -0.02 +0.09    -0.292 48.909
ATOM      2  C13 SUB dUNIT     30.323  40.032  -5.330 -0.08 -0.06    +0.170 48.909
ATOM      3  C16 SUB dUNIT     31.347  39.566  -6.307 -0.14 -0.02    +0.076 48.909
ATOM      4  C21 SUB dUNIT     31.480  40.239  -7.503 -0.15 -0.04    +0.085 48.909
ATOM      5  C28 SUB dUNIT     32.439  39.803  -8.418 -0.16 -0.01    +0.074 48.909
ATOM      6  C29 SUB dUNIT     33.243  38.704  -8.115 -0.13 +0.02    +0.071 48.909
ATOM      7  C27 SUB dUNIT     33.089  38.041  -6.897 -0.05 +0.02    +0.074 48.909
ATOM      8  C20 SUB dUNIT     32.130  38.478  -5.983 -0.11 +0.00    +0.085 48.909
ATOM      9  O3  SUB dUNIT     30.705  41.314  -7.820 -0.07 +0.47    -0.360 48.909
ATOM     10  H56 SUB dUNIT     30.928  42.054  -7.228 -0.48 -0.54    +0.217 48.909
ATOM     11  O4  SUB dUNIT     34.179  38.278  -9.007 -0.63 -0.20    -0.361 48.909
ATOM     12  H57 SUB dUNIT     33.733  37.800  -9.728 +0.04 +0.04    +0.217 48.909
ATOM     13  O2  SUB dUNIT     31.996  37.816  -4.800 -0.11 -0.03    -0.360 48.909
ATOM     14  H55 SUB dUNIT     31.234  37.217  -4.851 +0.04 +0.01    +0.217 48.909
ATOM     15  C5  SUB dUNIT     30.775  40.684  -4.048 -0.16 -0.02    +0.078 48.909
ATOM     16  C7  SUB dUNIT     30.997  42.190  -4.321 -0.31 -0.02    +0.034 48.909
ATOM     17  C8  SUB dUNIT     29.651  42.918  -4.537 -0.33 -0.03    +0.037 48.909
ATOM     18  C11 SUB dUNIT     28.525  42.435  -3.671 -0.21 +0.01    -0.023 48.909
```

```
ATOM     19  C9  SUB dUNIT     28.569  41.329  -2.907 -0.13 +0.02    -0.082 48.909
ATOM     20  C14 SUB dUNIT     27.416  40.988  -2.002 -0.12 -0.00    +0.043 48.909
ATOM     21  C6  SUB dUNIT     29.792  40.424  -2.876 -0.09 -0.00    +0.029 48.909
ATOM     22  C12 SUB dUNIT     31.915  42.808  -3.269 -0.31 +0.03    -0.053 48.909
ATOM     23  C17 SUB dUNIT     33.159  42.237  -3.018 -0.27 -0.00    +0.007 48.909
ATOM     24  C22 SUB dUNIT     33.998  42.802  -2.058 -0.45 -0.00    +0.001 48.909
ATOM     25  C24 SUB dUNIT     33.591  43.934  -1.354 -0.45 -0.00    +0.000 48.909
ATOM     26  C23 SUB dUNIT     32.342  44.502  -1.610 -0.37 -0.00    +0.001 48.909
ATOM     27  C18 SUB dUNIT     31.502  43.937  -2.570 -0.28 -0.00    +0.007 48.909
ATOM     28  C10 SUB dUNIT     29.445  38.930  -2.776 -0.05 -0.00    +0.037 48.909
ATOM     29  C15 SUB dUNIT     30.466  38.202  -1.963 -0.07 -0.00    -0.024 48.909
ATOM     30  C19 SUB dUNIT     30.708  36.877  -1.941 -0.06 -0.00    -0.091 48.909
ATOM     31  C25 SUB dUNIT     29.912  35.943  -2.814 -0.03 +0.00    +0.042 48.909
ATOM     32  C26 SUB dUNIT     31.752  36.202  -1.098 -0.08 +0.00    +0.042 48.909
TER
ENDMDL
```